UNIVERSITY OF BIRMINGHAM

DOES CROSSLINKING OF PODOPLANIN BY CLEC-2 INHIBIT MIGRATION OF LYMPHATIC ENDOTHELIAL CELLS?

&

REGULATION OF THE PLATELET COLLAGEN RECEPTOR GPVI AND ITS SHEDDASE ADAM10 BY TETRASPANIN MEMBRANE MICRODOMAINS

By

STACEY ANNE LANGAN

A thesis submitted to the University of Birmingham for the degree of

MASTER OF RESEARCH in BIOMEDICAL RESEARCH

Centre for Cardiovascular Sciences
College of Medical and Dental Sciences
University of Birmingham
August 2011

DOES CROSSLINKING OF PODOPLANIN BY CLEC-2 INHIBIT MIGRATION OF LYMPHATIC ENDOTHELIAL CELLS?

This project is submitted in partial fulfilment of the requirements for the award of the MRes

ABSTRACT

The platelet receptor CLEC-2 is a ligand for the transmembrane protein podoplanin, which is present on human lymphatic endothelial cells (HLEC). Mice lacking CLEC-2 or podoplanin display a blood-lymphatic mixing phenotype, possibly due to incomplete separation of the developing vessels. Previous work demonstrated that podoplanin mediates polarised migration of HLEC in response to VEGF-C and that platelets inhibit HLEC migration. Therefore, the aim of this work was to assess whether the interaction between podoplanin and CLEC-2 altered the migration of HLEC. Transfilter migration assays were used to assess the effect platelets and an anti-human podoplanin antibody on HLEC migration.

We found that platelets inhibit VEGF-C mediated HLEC migration in a count-dependent manner and that crosslinking podoplanin with a specific antibody and an appropriate secondary also gave a reduction in HLEC migration. Crosslinking podoplanin in the presence of the Rho kinase inhibitor Y27632 gave no further inhibition of migration. Using Y27632 in conjunction with platelets gave a partial recovery in the effect of platelets, suggesting platelets require activation of the RhoA signalling pathway to exert their anti-migratory effects.

In summary, crosslinking podoplanin with platelets or antibodies inhibits VEGF-C mediated HLEC migration and this may be dependent on the RhoA signalling pathway.

ACKNOWLEDGEMENTS

Firstly, I would like to thank my supervisors, Gerard Nash and Steve Watson, for their guidance and support throughout the time I have worked with them.

Thanks also go to all members of the Watson group for making me feel welcome in a new lab, but particularly to Leyre Navarro-Núñez, for day-to-day supervision, teaching me the techniques I used throughout the project and generally being a source of support and advice during my time in the Watson lab.

Finally, thanks go to my family, Kevin, Pat and Jamie Langan and my partner, Adam Baggett, whose support and encouragement have been invaluable over the past months.

TABLE OF CONTENTS

1. INTRODUCTION

1.1. The lymphatic system & lymphangiogenesis

The lymphatic system is a complex network of vessels whose functions are (i) to return tissue fluid exuded from the blood vessels to the circulation; (ii) to absorb lipids in the intestinal villi; and (iii) to transport leukocytes and antigen-presenting cells to secondary lymphoid tissues as part of the immune response. Therefore, tissues which are in frequent contact with foreign antigens, such as the skin and mucous membranes, have noticeably higher numbers of lymphatic vessels.

The structure and permeability of lymphatic vessels is distinct from that of blood vessels. This is particularly apparent in the lymphatic capillaries, which are formed from a single layer of lymphatic endothelial cells (LEC). LEC have little or no basement membrane and loose intercellular junctions, which makes the lymphatic capillaries highly permeable and allows leukocytes to enter the lymphatic vessels (1), whereas blood vascular endothelial cells (BVEC) have tight intercellular junctions, making them significantly less permeable. In contrast to BVEC, which are supported by pericytes and smooth muscle cells, LEC are only stabilised by anchoring filaments (2), which connect LEC to the extracellular matrix and dilate the lumen of the lymphatic capillary as interstitial pressure increases, enhancing the uptake of tissue fluid (1). While this structure applies to lymphatic capillaries, the larger lymphatic collecting vessels can have smooth muscle cells, continuous interendothelial junctions and basement membranes.

LEC express several specific markers not found in BVEC but expressed separately by some non-endothelial cells (3), including the transcription factor prospero-related homeobox 1 (Prox1), vascular endothelial growth factor receptor 3 (VEGFR3) and the transmembrane protein podoplanin. All of these markers have specific roles in lymphatic development.

The lymphatic system develops once the blood vascular system is established and functional. This occurs at around week 6-7 in human embryonic development and at embryonic day (E) 9.5-10.5 in mice (1) when a subpopulation of endothelial cells in the cardinal vein begin expressing Prox1, which commits them to the lymphatic lineage (Figure 1). In Prox1-deficient embryos, these cells fail to express lymphatic endothelial markers and instead retain their blood vascular endothelial phenotype (4). The result of this deficiency is that lymphatic vessels and lymph sacs do not develop (5-7).

This Prox1-positive subpopulation of cells begin to show a LEC phenotype with an increase in the expression of other LEC markers, such as podoplanin and VEGFR3, with a simultaneous decrease in BVEC markers, including CD34 and laminin (5). During this process there is a reduction in the vein's pericyte and smooth muscle coverage (8) that, when combined with degradation of the extracellular matrix, allows LEC to access the mesenchyme (9). Vascular endothelial growth factor C (VEGF-C) is synthesised by the surrounding mesenchyme (10) and interacts with both VEGFR2 and VEGFR3, although with higher affinity for VEGFR3 (11). It promotes LEC sprouting and directional migration, leading to the formation of primordial lymph sacs (11). Blocking VEGF-C is known to prevent lymphangiogenesis through a failure in LEC migration (12,13).

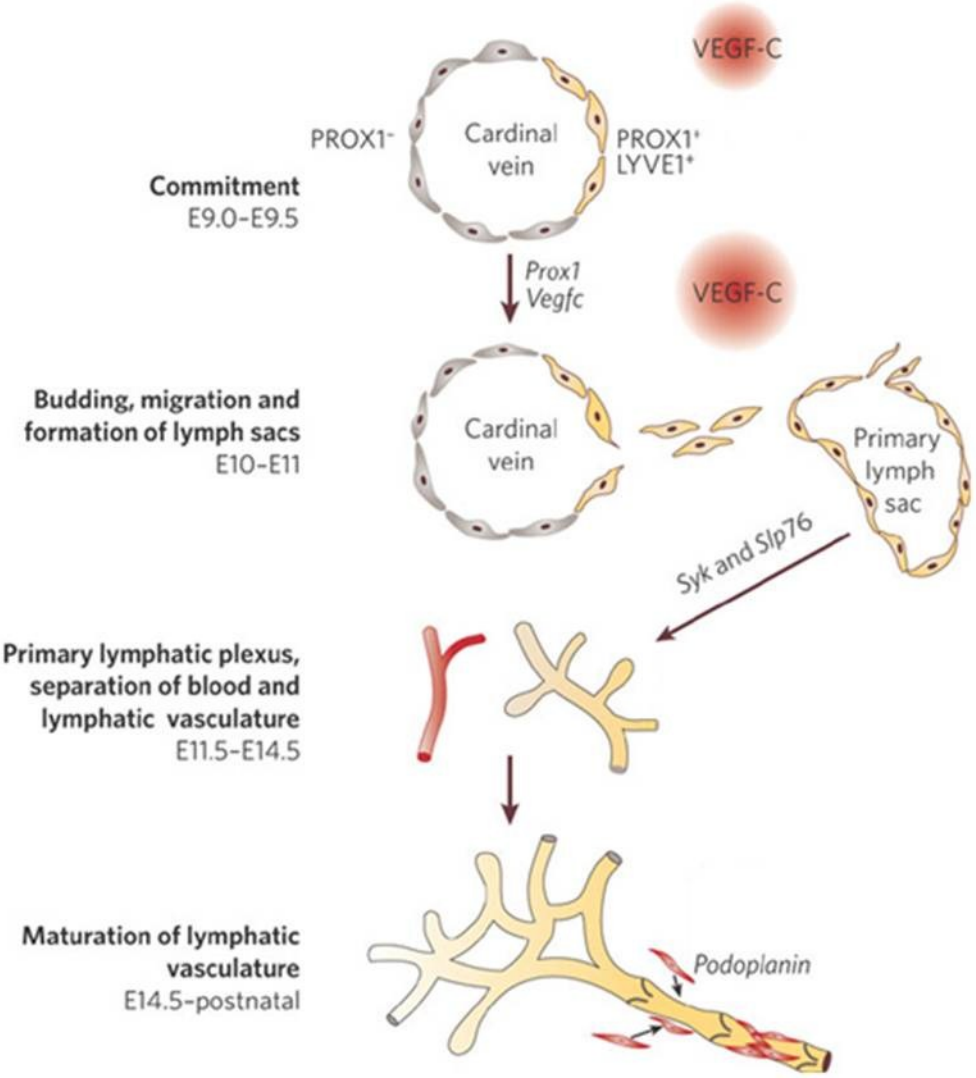

Figure 1: Overview of lymphangiogenesis in a mouse model. At E9.5 cells on one side of the cardinal vein begin expressing Prox1, which signals their commitment to the lymphatic lineage. These cells then begin expressing additional LEC markers, including podoplanin and VEGFR3, before migrating away from the cardinal vein. This migration is dependent on VEGF-C and leads to the formation of the primary lymph sacs. The blood and lymphatic systems separate between E11.5 and E14.5. This is thought to involve platelet signalling via Syk and SLP-76. Adapted from (17).

LEC migration is characterised by reorganisation of the actin cytoskeleton, which allows lamellipodia to be extended and the edge of the cell to bind to the substratum. From this point the cell body is moved forwards before it detaches from the substratum and the tail end of the cell is retracted (14). VEGF-C is also known to promote LEC proliferation (15), required for the growth of lymph sacs and generation of a network of lymphatic vessels, which can be detected throughout the embryo by E14.5 (16).

Lymphangiogenesis can also occur in a number of pathologies. It can be associated with acute or chronic inflammation, such as at sites of bacterial infection or in rheumatoid arthritis (17). In these circumstances macrophages and granulocytes at the inflammatory site produce VEGF-C, promoting the generation of lymph vessels (13,17). Lymphangiogenesis also occurs during tumour metastasis, particularly in breast and colon carcinomas. Metastasis via the lymphatic system is the most common form of metastasis for solid tumours (18). Tumour cells are able to produce lymphangiogenic factors, including VEGF-C, which allow the development of peritumoural lymphatic vessels and facilitate lymphatic metastasis (19).

1.2. Podoplanin

Podoplanin has recently been identified as a surface receptor on LEC, but has not been found on BVEC. It is a heavily glycosylated small transmembrane protein that is also expressed by kidney podocytes, type 1 lung alveolar cells, osteoblasts and epidermal keratinocytes (3). Podoplanin can be detected in the cardinal vein from E11.5 in mice and later becomes restricted to Prox1-expressing LEC in the developing lymph sacs (20,21). Podoplanin-deficient mice die from respiratory failure shortly after birth and are known to

have incomplete formation of lymphatic, but not blood vessels (21,22). Endothelial loss of the T-synthase enzyme, required for the correct O-glycosylation of podoplanin, also leads to embryonic and neonatal lethality associated with disorganised and blood-filled lymphatic vessels (23).

Although the role of podoplanin is not yet completely understood, there is considerable evidence of its role in regulating cell migration. Podoplanin can bind through its cytoplasmic tail to ezrin/radixin/moesin (ERM) proteins, which connect actin filaments and the cell membrane and subsequently activate RhoA GTPases (24). The Rho GTPases are a family of signalling molecules that control a number of cellular processes, including the cytoskeletal rearrangements necessary for polarised cell migration. These proteins can exist in both GTP-bound active and GDP-bound inactive states and conversion between these is regulated by guanine nucleotide-exchange factors, GTPase-activating proteins and guanine nucleotide-dissociated inhibitors (25). Activated GTPases bind to a range of different effector molecules, including Rho kinase, which is associated with the regulation of cell contraction and the formation of stress fibres (26). RhoA signalling has previously been shown to be involved in VEGF-induced migration of BVEC (27) and it has recently been reported that polarised migration of human lung microvascular LEC requires the regulation of RhoA by podoplanin (28). Moreover, podoplanin upregulation in tumours is associated with altered actin cytoskeleton reorganisation and increased metastasis (24), whereas siRNA-mediated knockdown of podoplanin causes a dramatic reduction in directional migration (28). These effects appear to be independent of ligand engagement and may therefore reflect constitutive signalling from podoplanin. Whether the binding of a ligand to podoplanin alters this signalling remains to be proved.

1.3. Platelets in lymphatic development

Similar to T-synthase or podoplanin knockouts, mice deficient in SYK, SLP-76 or PLCγ-2 develop a blood-lymphatic mixing phenotype (29-31). Together with the identification of podoplanin as the endogenous ligand for the platelet membrane protein C-type lectin receptor 2 (CLEC-2) (32,33), these studies led to the proposal that correct separation of the lymphatic and blood vessels requires interaction between podoplanin on LEC and CLEC-2 on platelets, resulting in CLEC-2 signalling through Syk, SLP-76 and phospholipase Cγ2 (PLCγ2).

CLEC-2 is a type II transmembrane protein primarily expressed by platelets and megakaryocytes (34,35), but has also been identified in immune cells such as mouse neutrophils (36). This platelet receptor, which exists on the surface of platelets as a dimer (35,37), was first identified as a receptor for the snake venom toxin rhodocytin (34). CLEC-2 also mediates tumour cell-induced platelet activation by interacting with podoplanin on the tumour cell surface and is known to contribute to tumour metastasis (33,38).

The cytosolic tail of CLEC-2 contains a conserved YxxL sequence known as a hemITAM, preceded by three acidic amino acids (DED). When a ligand (podoplanin, rhodocytin or specific antibodies) binds to the receptor, the tyrosine of the hemITAM motif is phosphorylated, creating binding sites for the SH2 domains of the tyrosine kinase Syk (35). Once Syk has bound to CLEC-2 it is phosphorylated by Src family kinases, resulting in the activation of PLCγ2 and a potent platelet aggregation and secretion response (34).

CLEC-2 knockout mice die shortly after birth and embryos show haemorrhage, oedema and a blood-lymphatic mixing phenotype similar to that seen in podoplanin-deficient mice. It has also been noted that the lymphatic vessels in CLEC-2 knockout

embryos are more dilated and appear rugged when compared to the same vessels in normal embryos (39). As podoplanin is the only known endogenous ligand for CLEC-2, the phenotype of these mice confirmed the hypothesis that the interaction between CLEC-2 and podoplanin is required for normal lymphatic development.

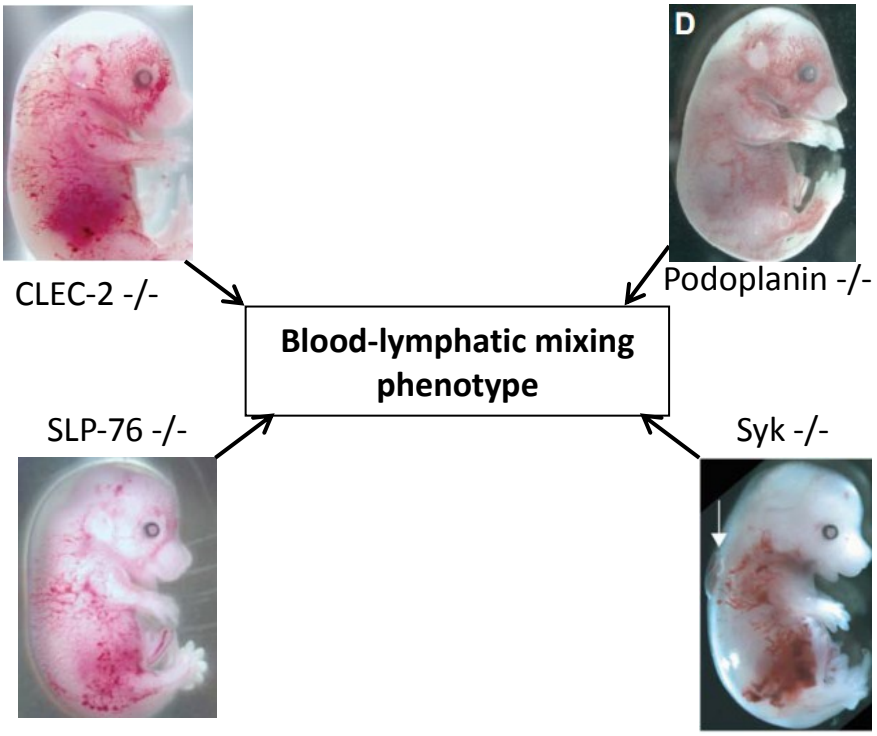

Figure 2: Mice lacking proteins associated with CLEC-2 signalling display the same phenotype. Mice deficient in CLEC-2, podoplanin, SLP-76 or Syk all display a blood-lymphatic mixing phenotype. This is thought to be due to incomplete separation of the developing vascular systems. Adapted from (21,22,29,39).

1.4. Hypothesis and aims of the project

Mice deficient in either podoplanin or CLEC-2 develop a blood-lymphatic mixing phenotype that suggests the two systems are not properly separating during embryonic development (21,39). In addition to this, previous work has shown that a high number of platelets reduce the migration of LEC (Navarro-Núñez et al., unpublished data). The LEC surface protein podoplanin is the only known endogenous ligand for the platelet receptor CLEC-2 (34). Therefore it was hypothesised that the crosslinking of podoplanin would prevent LEC migration. The specific aims of this project were to assess whether (i) platelet-mediated or (ii) antibody-mediated crosslinking of podoplanin inhibits LEC migration. This was achieved by assessing LEC migration in transfilter assays in the presence of platelets or an anti-human podoplanin antibody.

2. METHODS

2.1. Cell culture

Primary human dermal lymphatic endothelial cells (HLEC) were obtained from PromoCell (Heidelberg, Germany). The cells were maintained in 1% gelatine-coated flasks with MV2 basal medium that was supplemented with: 50 µl/ml foetal calf serum, 5 ng/ml recombinant human epidermal growth factor, 10 ng/ml recombinant human basic fibroblast growth factor, 20 ng/ml insulin-like growth factor (long R3 IGF-1), 0.5 ng/ml recombinant human vascular endothelial growth factor 165, 1 µg/ml ascorbic acid and 0.2 µg/ml hydrocortisone (PromoCell). For cell passage HLEC were detached with 0.05% trypsin-EDTA (PAA, Yeovil, UK) when confluent, while non-enzymatic dissociation solution (Sigma, Poole, UK) was used to prepare cells for experiments.

2.2. Preparation of washed human platelets

Whole blood was obtained from healthy volunteers who had not taken any medication affecting platelet function in the previous 10 days. Informed consent was obtained before donation and blood was drawn into 4% sodium citrate (1/9 volume). To further prevent activation of isolated platelets, 10% acid citrate dextrose (ACD: 120 mM sodium citrate, 110 mM glucose and 80 mM citric acid) was added to the blood, which was centrifuged at 200 g for 20 minutes. The resulting platelet rich plasma (PRP) was pipetted into a clean 50 ml Falcon tube. 2.84 µM prostacyclin was added; the tube was mixed by inversion and centrifuged at 1000 g for 10 minutes. The pellet was resuspended in 1 ml modified Tyrode's buffer (134 mM NaCl, 2.9 mM KCl, 0.34 mM Na_2HPO_4, 12 mM $NaHCO_3$, 20 mM HEPES, 1 mM $MgCl_2$; pH 7.3), then 24 ml modified Tyrode's buffer, 3 ml ACD and 2.84

µM prostacyclin were added to the tube, which was centrifuged at 1000 g for a further 10 minutes. The pellet was resuspended in 1 ml modified Tyrode's and the cells were counted using a cell counter (Coulter, High Wycombe, UK) before being diluted to the required concentration. Platelets were allowed to rest for at least 30 minutes before the start of an experiment.

2.3. Flow cytometry

Flow cytometry was used to confirm the presence of podoplanin on the surface of HLEC. Cells were detached from the flask using a non-enzymatic solution and resuspended in sterile PBS (Invitrogen, Paisley, UK). $4x10^4$ HLEC in 75 µl were added to FACS tubes and incubated with 2.5 µg/ml of phycoerythrin-conjugated rat anti-human podoplanin (clone NZ-1.3) or phycoerythrin-conjugated rat IgG2a isotype control (eBioscience, Hatfield, UK) following the manufacturer's instructions. After the cells were incubated with the respective antibodies for 30 minutes in the dark, 300 µl PBS was added to each tube before the samples were analysed on a FACSCalibur flow cytometer (BD Bioscience, Oxford, UK) using Cellquest with voltage settings as follows: forward scatter (FSC): E-01; side scatter (SSC): 211; both in log mode. Data was collected from 10,000 events for each sample and a gate was applied around live cells for analysis.

An indirect FACS staining approach using the same antibody clone (NZ-1.3) or a rat IgG control (R&D Systems, Abingdon, UK) followed by an Alexa Fluor 488 goat anti-rat IgG secondary also showed specific podoplanin staining in HLEC. To determine the saturating concentration of the unconjugated NZ-1.3 antibody, $4x10^4$ HLEC in 75 µl were stained with serial dilutions of the antibody in PBS to give final concentrations ranging from 5 to 0.15625

µg/ml. Two rat IgG controls were prepared in parallel at final concentrations of 2 or 20 µg/ml. The secondary antibody was kept at a fixed concentration of 25 µg/ml. After incubation with the secondary antibody the samples were diluted with 300 µl PBS and analysed as above.

2.4. Cell migration assay

Migration assays used 24-well plates with cell culture inserts (BD Biosciences, Oxford, UK; 8µm pore size). To assess the best time point for the experiment, initial assays used incubation periods of 24 and 48 hours. In these preliminary experiments the effect of VEGF-C on HLEC migration was assessed by adding 0, 150 or 300 ng/ml VEGF-C (R&D Systems) in cell culture medium to the lower chamber of the well. $3x10^4$ HLEC in complete culture medium were applied to the upper chamber of the insert in a volume of 200 µl. After incubation for the indicated time points at 37 °C and 5% CO_2, the VEGF-C solutions and medium were removed from both chambers and the inserts were washed with sterile PBS. A fixative solution consisting of 2% buffered formalin (Sigma) in sterile PBS with 2 µg/ml bisbenzimide (Sigma) was applied to the inserts (700 µl in the lower chamber and 300 µl in the upper chamber). The inserts were incubated at room temperature, protected from light, for 15 minutes before the fixative was removed and the inserts washed with PBS. The porous membranes were cut out of each insert and mounted onto a microscope slide using Hydromount (National Diagnostics, Georgia, USA), a non-fluorescent mounting medium. All slides were stored in the dark at 4°C until visualisation.

In later experiments the effect of platelets on HLEC migration in the presence and absence of VEGF-C was examined. HLEC were applied to the insert as before and incubated

at 37°C for one hour before washed human platelets were added. $1x10^4$ – $1x10^8$ platelets in modified Tyrode's were added to the filter in volumes of 100 µl. The same volume of buffer was added to non-treated parallel controls. In separate experiments, to assess whether platelet addition might affect HLEC adhesion to the porous membrane, platelets were added to the insert immediately after HLEC seeding or an hour later. This experiment was performed in the presence of VEGF-C and the final incubation time was 24 hours.

The effect of the rat anti-human podoplanin antibody NZ-1.3 on VEGF-C induced HLEC migration was also examined. NZ-1.3 antibody was applied to the insert at a concentration of 2 µg/ml and in some wells an anti-rat IgG2a antibody (Biolegend, Bar Hill, UK) was also added at different ratios to induce crosslinking. The negative controls contained 2 µg/ml of an irrelevant rat IgG with and without the anti-rat secondary antibody.

In separate experiments wells were set up with 100 µM of the Rho kinase inhibitor Y27632 (Calbiochem, Nottingham, UK) or PBS as a control. This inhibitor was also used in combination with 10^8 platelets or 2 µg/ml anti-human podoplanin antibody. The aim of these experiments was to determine whether inhibiting a downstream effector of RhoA would inhibit VEGF-C mediated HLEC migration and to assess whether Rho kinase was involved in the mechanism underlying the effects seen with platelets and the anti-human podoplanin antibody.

2.5. Microscopy

The results of the cell migration assay were analysed by visualising the stained HLEC nuclei using an inverted fluorescent microscope (Zeiss, Hertfordshire, UK) and counting the

number of cells above and below the filter in 15 separate fields per insert. Percentage transmigration was calculated as follows:

$$\text{Percentage migration} = \frac{Number\ of\ migrated\ cells}{Total\ number\ of\ cells} \times 100$$

2.6. Evaluation of success of podoplanin crosslinking

2.6.1. Sample Preparation

Platelets were isolated from whole blood as outlined above and were diluted in modified Tyrode's solution to give a concentration of $1x10^9$/ml. Non-enzymatically detached HLEC were resuspended in sterile PBS at a concentration of $5x10^5$ cells/ml. Crosslinking of podoplanin was then attempted using either antibodies or platelets. The cells undergoing antibody-mediated crosslinking were incubated with either 10 µg/ml of an anti-human podoplanin antibody or rat IgG. After incubating for 30 minutes on ice an anti-rat secondary antibody was added to two of the tubes. The control sample contained HLEC with PBS. The cells used for platelet-mediated crosslinking were incubated for 30 minutes at 37 °C under stirring with washed human platelets or washed platelets that had been fixed in 1% formaldehyde.

Once the samples had been incubated with the appropriate combination of antibodies or platelets, sulfo-EGS (Thermo Scientific, Loughborough, UK) was added to each sample at a final concentration of 1.5 mM. This chemical crosslinker was used to stabilise any platelet or antibody-mediated crosslinking that had occurred. The samples were incubated at room temperature for 30 minutes before 1 M Tris-HCl was added at a final

concentration of 25 mM to quench the reaction between the samples and sulfo-EGS. The samples were incubated for a further 20 minutes at room temperature. Next, an equal volume of 2x ice-cold lysis buffer (50 mM Tris, 150 mM NaCl, 1 mM EDTA, 1 mM EGTA, 0.5 mM AEBSF, 1 mM Na_3VO_4, 5 mM NaF, 1 µg/ml pepstatin A, 5 µg/ml aprotinin, 5 µg/ml leupeptin, 1% NP-40) was added to the samples, which were centrifuged for 10 minutes at 13,000 rpm with the centrifuge set to 4 °C. The samples were then stored at -20 °C until analysis by Western blot at a later date.

2.6.2. SDS-PAGE and Western blot

Proteins in the samples were resolved by 10% polyacrylamide gel electrophoresis under reducing conditions. The stacking buffer used consisted of 0.5 M Tris-HCl at pH 6.8, while the resolving buffer was 3 M Tris-HCl at pH 8.8. 32 µl of each sample was mixed with 8 µl of 5x Laemmli buffer (10% SDS, 25% 2-mercaptoethanol, 50% glycerol, 25% stacking buffer, trace Brilliant Blue R). The samples were boiled for five minutes at 100 °C then centrifuged briefly. 10 µl of a molecular weight marker (New England Biolabs, Hitchin, UK) was loaded onto the gel, followed by 30 µl of each sample in consecutive wells. The tank was filled with running buffer (25 mM Tris, 192 mM glycine, 0.1% SDS) and run at 100 V for approximately 2 hours. Proteins were then transferred to a PVDF membrane (Biorad, Hemel Hempstead, UK) previously soaked in methanol, water and cold transfer buffer (48 mM Tris, 39 mM glycine, 1.3 mM SDS, 20% methanol) inside a transfer cassette with the membrane and gel sandwiched between filters pre-soaked in transfer buffer.

The transfer cassette was set up with the membrane and gel sandwiched between the pre-soaked filters. The transfer was run at 100 mA for 40 minutes. After the transfer

had completed the gel and filters were discarded. The membrane was blocked in 10% bovine serum albumin (BSA) containing 0.1% sodium azide in TBS-T (200 mM Tris, 1.37 M NaCl, 0.1% Tween-100) for an hour. An anti NZ-1.3 antibody (1/5000 dilution) was prepared in 10 ml 10% BSA in TBS-T. The blocking BSA was removed from the membrane and replaced with this antibody solution, which was left on the membrane overnight on a rocking platform at 4°C.

The membrane was then washed three times in TBS-T, for 20 minutes each time on a rocking platform. A 1/10000 dilution of horseradish peroxidase (HRP)-conjugated anti-rat antibody (Santa Cruz Biotechnology, Heidelberg, Germany) was prepared in 10 ml TBS-T. The membrane was incubated with this antibody solution for an hour at room temperature, before being washed as before. Finally, the membrane was washed briefly with water and excess liquid was blotted from the membrane. 1 ml of each solution from an enhanced chemiluminescence detection kit (Thermo Scientific, Loughborough, UK) was applied to the membrane, left for one minute and excess removed. The membrane was developed using autoradiography with an exposure time of 30 minutes.

2.7. Statistics

The Student's t-test was used to determine the significance between data sets. Where several conditions needed to be compared, an analysis of variance (ANOVA) was performed to determine statistical significance.

3. RESULTS

3.1. Podoplanin is present on the surface of lymphatic endothelial cells

When purchased, the HLEC are described as expressing podoplanin on their surface. To confirm this before the cells were used in any experiments, flow cytometry was performed with the cells stained for podoplanin using both direct and indirect methods. Gating around intact cells showed that podoplanin was expressed on the surface of HLEC (Figure 3B &D) and that staining with an irrelevant isotype-matched rat IgG showed low levels of non-specific staining (Figure 3A & C). In contrast, when a gate was applied to the cell debris the samples incubated with anti-human podoplanin showed a low level of podoplanin staining, while incubation with IgG confirmed a low level of background signal (Figure 4A-D). The levels of podoplanin staining were quantified using the mean fluorescence intensity of each sample (Figure 5). The level of fluorescence after indirect staining with rat IgG appears high in the cell debris (Figure 5B), but this level of staining was consistent with the fluorescence seen in the indirectly stained intact cells and was still much lower than the fluorescence seen in the intact samples stained with anti-human podoplanin (Figure 5A).

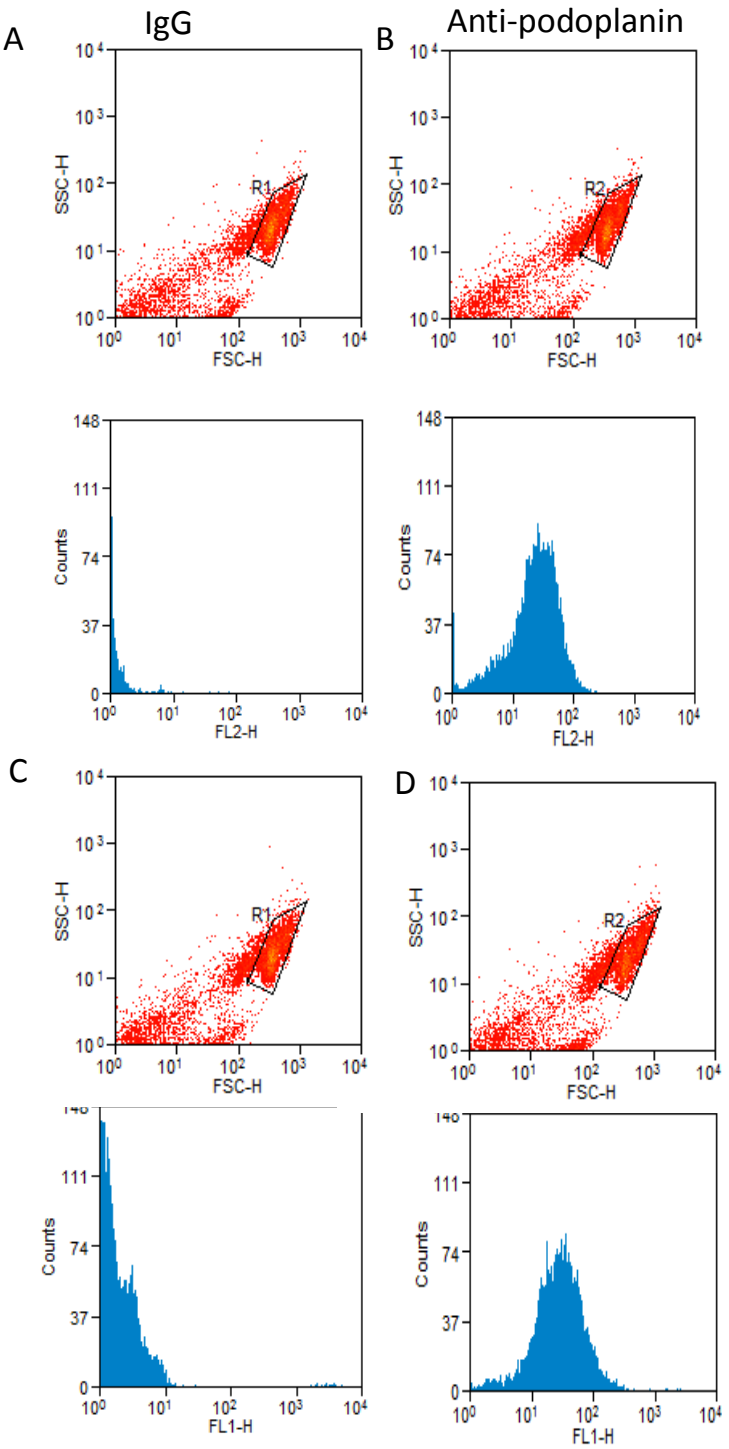

Figure 3: Podoplanin is present on the surface of HLEC. Direct staining using phycoerythrin-conjugated IgG showed a low level of background staining (A) but using a phycoerythrin-conjugated anti-human podoplanin antibody showed the presence of podoplanin on the surface of HLEC (B). Similarly, indirect staining of HLEC with rat IgG showed a low level of non-specific stining (C), while staining with anti-human podoplanin showed the presence of podoplanin on HLEC (D).

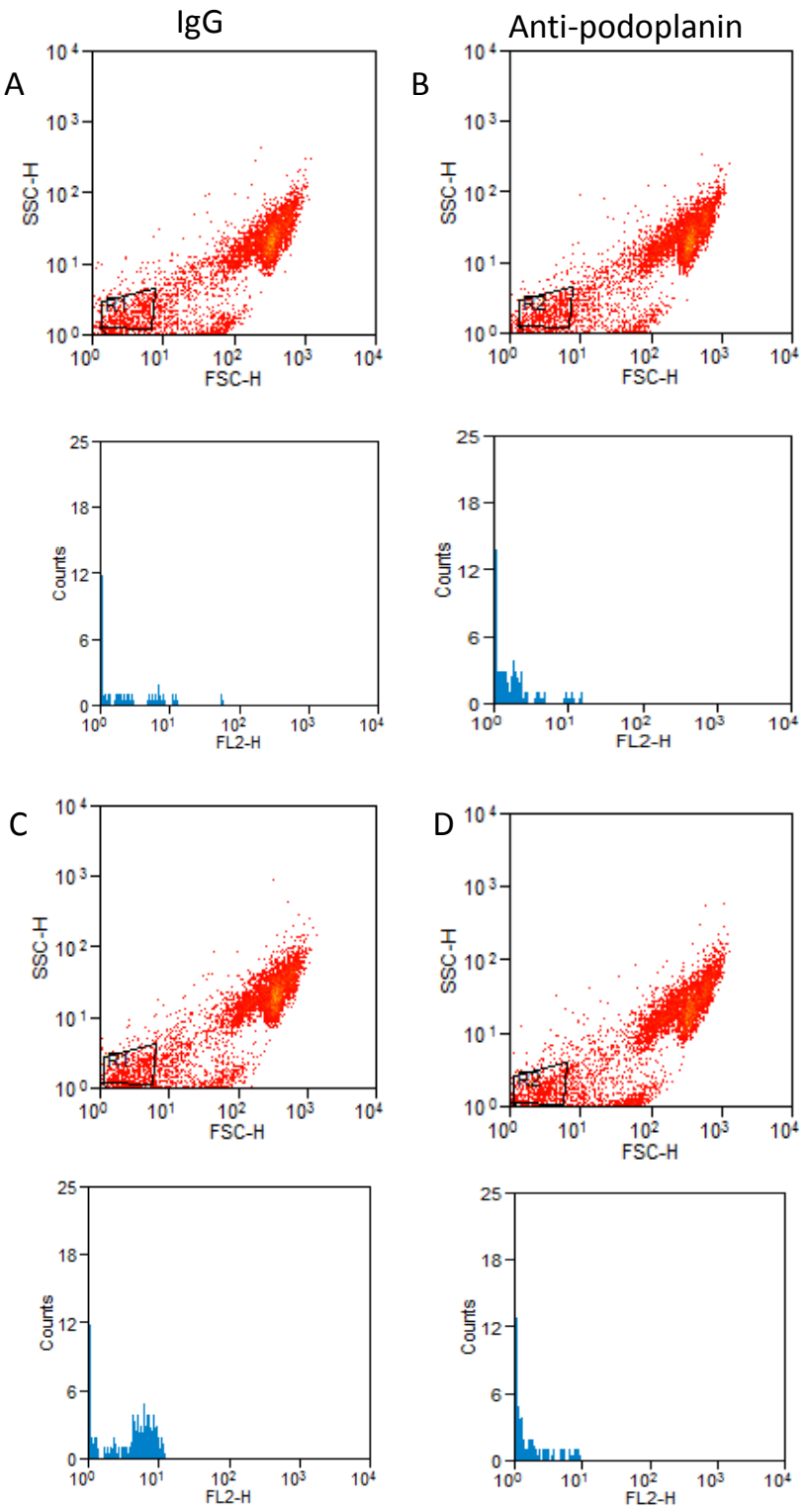

Figure 4: Podoplanin is not present in the cell debris. Using the same samples as previously, the cell debris was gated to determine whether podoplanin was present. Neither of the directly stained samples (A and B) showed any podoplanin in the cell debris. The indirect samples (C and D) showed some low levels of staining, which may be due to the background noise in the samples. The alternative explanation is that there were fragments of HLEC membrane containing podoplanin in the debris.

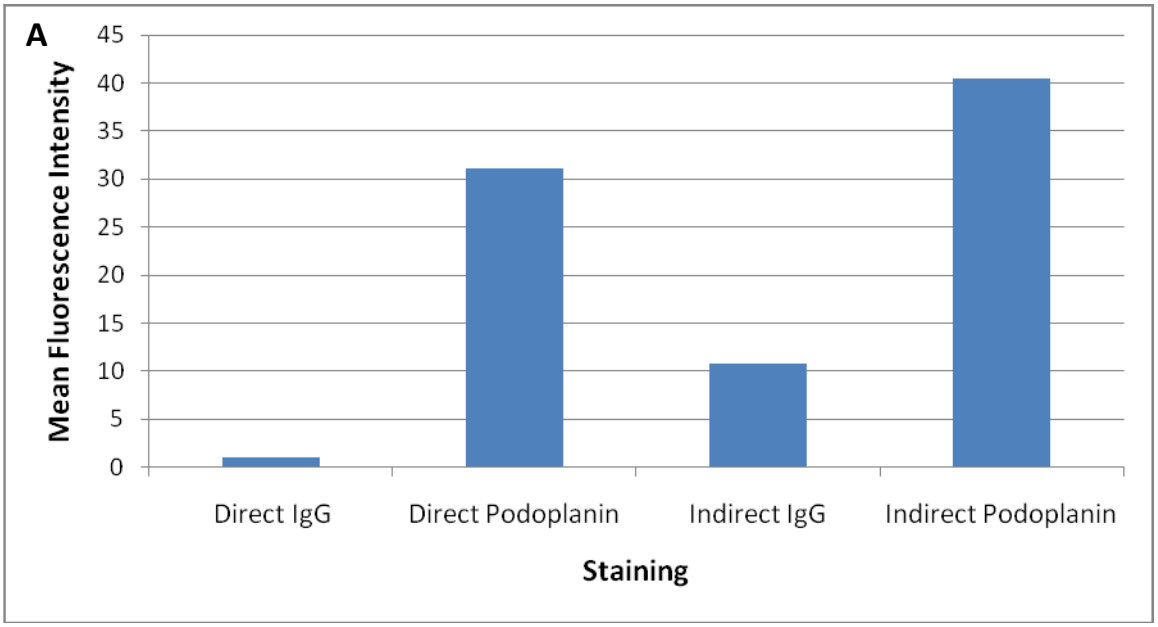

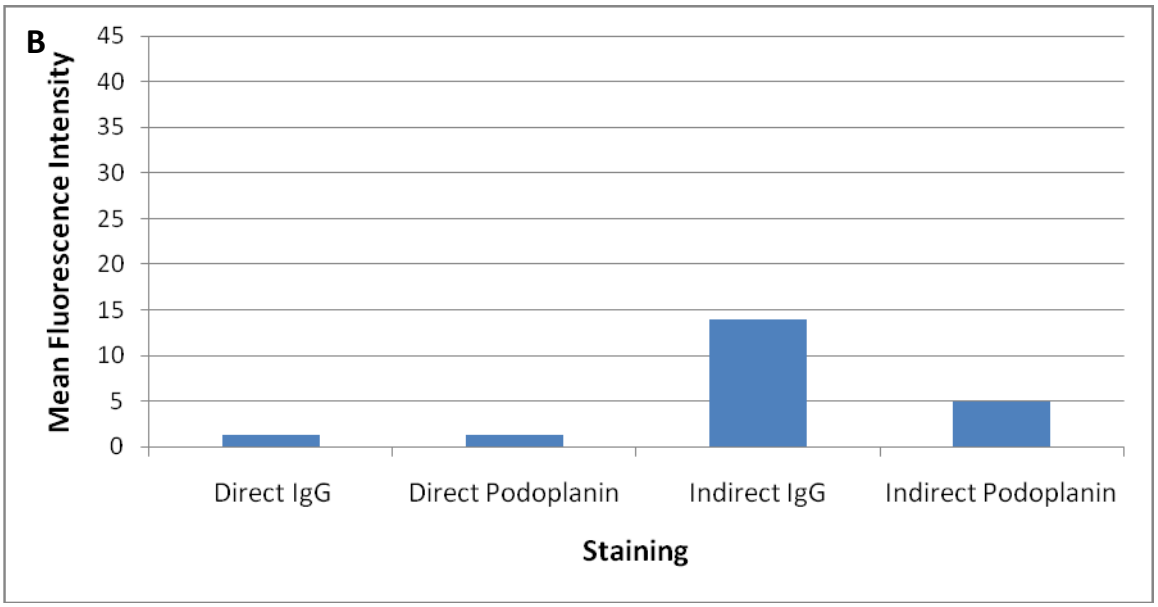

Figure 5: Quantification of podoplanin staining in intact HLEC and cell debris. The mean fluorescence intensity was determined in both intact HLEC and cell debris. (A) The intact cells showed an increase in fluorescence when staining was performed with anti-human podoplanin. (B) The cell debris showed low levels of fluorescence with both rat IgG and anti-human podoplanin. While the indirect IgG sample appears to have a high level of fluorescence this is actually similar to the background fluorescence seen in the intact cells (MFI = 13.91 vs 10.82) and is still much lower than the fluorescence seen with podoplanin staining in intact HLEC. n = 1

3.2. Platelets reduce VEGF-C mediated migration of lymphatic endothelial cells

Having confirmed that podoplanin was present on HLEC, modified Boyden chamber assays were performed to assess transmigration of HLEC. This assay allows quantitation of cell migration through a porous membrane and reagents can be added to the assay to assess their effect on migration. In this study, VEGF-C was used in the assay as it has been shown to promote directional HLEC migration (12,13). The assay was characterised to determine the most appropriate incubation time and concentration of VEGF-C. The incubation times used in these preliminary experiments were 24 and 48 hours and the lower chamber of the wells contained 0, 150 or 300 ng/ml VEGF-C diluted in normal cell culture medium. These concentrations (corresponding to 0, 10 and 20 nM respectively) were selected as they were close to the dissociation constant (K_D, ligand concentration at which 50% of receptors are occupied) of the VEGFR-2 and VEGFR-3 receptors (Table 1), which are both receptors for VEGF-C (11). Additionally, a previous report showed that 15 nM VEGF-C is within the maximal proliferation response range for both HUVEC and MEC (microvascular endothelial cells) and is near the peak migratory response for these cells (40).

At 24 hours, VEGF-C increased the migration rate in a concentration-dependent manner, while at 48 hours HLEC migration was similar in all wells (Figure 6), which was probably due to both VEGF-C and HLEC reaching equilibrium. Therefore, it was decided that for future experiments an incubation time of 24 hours would be used as the assay loses sensitivity to VEGF-C at 48 hours. Preliminary experiments (Navarro-Núñez et al.,

unpublished data) showed that platelets inhibit HLEC migration. Therefore, the experimental conditions had to give a high level of migration in the absence of platelets to allow a decrease to be detected. The data obtained in these experiments suggested that 300 ng/ml VEGF-C would give a percentage migration of approximately 40% without platelets, making any decrease in migration possible to identify, whilst being different from the migration seen without VEGF-C.

Ligand	**Receptor**	**K_D (M)**	**Reference**
hVEGF-C	hVEGFR-2	2.2×10^{-8}	Mäkinen et al., 2001
hVEGF-C	hVEGFR-3	0.44×10^{-8}	Mäkinen et al., 2001

Table 1: Dissociation constants (K_D) for VEGF-C at its known receptors. VEGF-C is known to bind to both VEGFR-2 and VEGFR-3, but has been shown to have a higher affinity for VEGFR-3 (Mäkinen et al., 2001). VEGFR-2 and VEGFR-3 K_D values for VEGF-C are shown. 150 ng/ml and 300 ng/ml VEGF-C correspond to 9.68×10^{-9} and 1.94×10^{-8} M, respectively. These concentrations are close to the K_D values of VEGFR-3 and VEGFR-2 for VEGF-C.

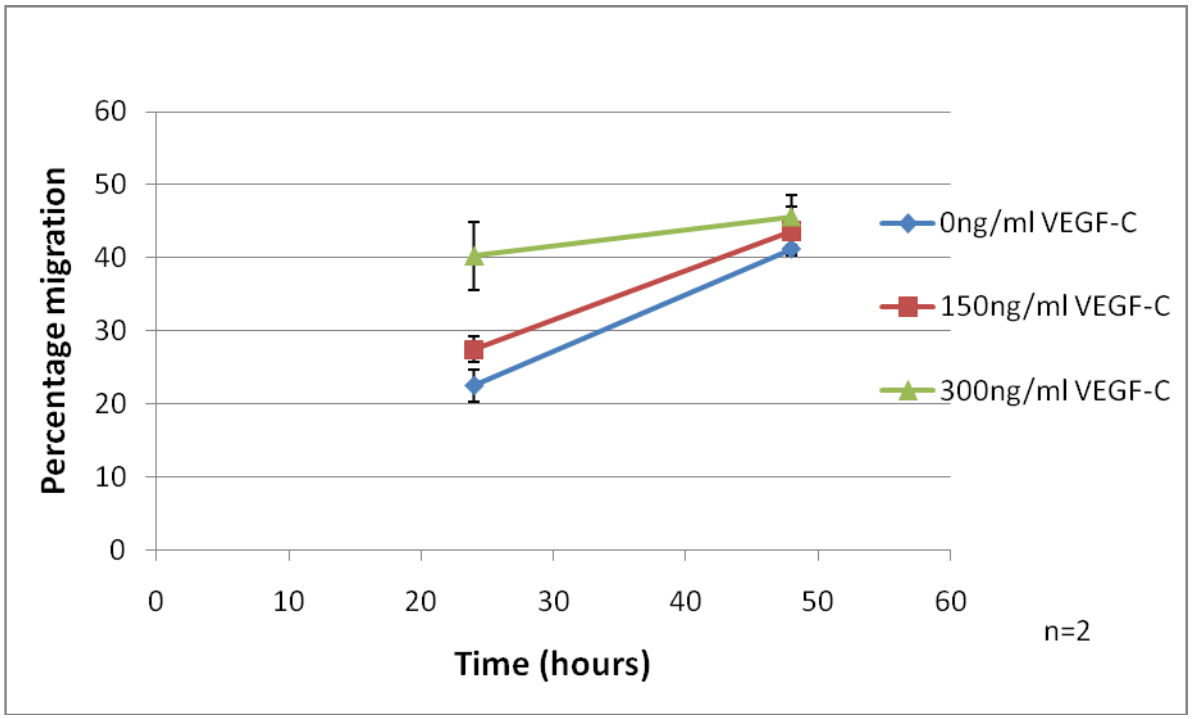

Figure 6: Characterisation of the transfilter migration assay: Cell culture inserts with 8 µm pores were placed into the wells of 24-well plates. The lower chambers of the wells were filled with complete culture medium containing 0 ng/ml, 150 ng/ml or 300 ng/ml VEGF-C. 3 x 10^4 HLEC in a volume of 200 µl were added to the filter and the wells were incubated for 24 or 48 hours. After incubation, the porous membranes were washed, fixed, stained and mounted. Percentage migration was calculated in fifteen fields by dividing the number of cells counted in the bottom chamber by the total number of cells counted. Error bars represent the standard deviation of two independent experiments.

The effect of human platelets on HLEC transmigration in the presence or absence of 300 ng/ml VEGF-C was assessed by performing cell migration assays with differing numbers of platelets applied to the upper well of the chamber. HLEC were added in a volume of 200 µl and allowed to settle for an hour before the addition of platelets or modified Tyrode's solution to exclude a potential effect of platelets on attachment of HLEC to the membrane. The number of platelets used in each well varied from 10^4-10^8 in a volume of 100 µl. A healthy adult has approximately 1.5 - 4 x 10^7 platelets in 100 µl blood, so the platelet counts used here were not excessive. This experiment confirmed that platelets inhibit HLEC

migration and showed that this was specific to VEGF-C mediated migration (Figure 7A & B). A two-way analysis of variance (ANOVA) confirmed that the addition of platelets to the assay was significantly inhibiting migration ($P = 0.001$) and that this effect was only significant in the presence of the chemokinetic VEGF-C ($P = 0.001$). These data suggest that the presence of platelets alters the migratory potential of HLEC in response to VEGF-C. At the two highest platelet counts, the migration levels seen with and without VEGF-C were similar (Figure 7B), suggesting that the basal rate of migration was not affected by platelets.

It was suggested that the addition of platelets may affect the viability and/or adhesion of the HLEC. To test this, the transmigration assays were repeated with 10^8 platelets added either immediately after HLEC or after the cells had been incubated for an hour. Analysis of the filters showed that adding platelets at t=0 hours or t=1 hour had the same inhibitory effect on HLEC migration through the filter (Figure 8A). In addition to calculating the percentage of migration, the average number of cells on each filter was also recorded. This showed that there was no significant difference between the number of cells on each filter, regardless of treatment (Figure 8B), suggesting that platelets were not preventing the HLEC adhering to the filter or increasing cell death. Although adding platelets immediately after HLEC did not alter percentage migration or the number of cells on each filter, future experiments retained the hour-long incubation period to maintain continuity throughout the study.

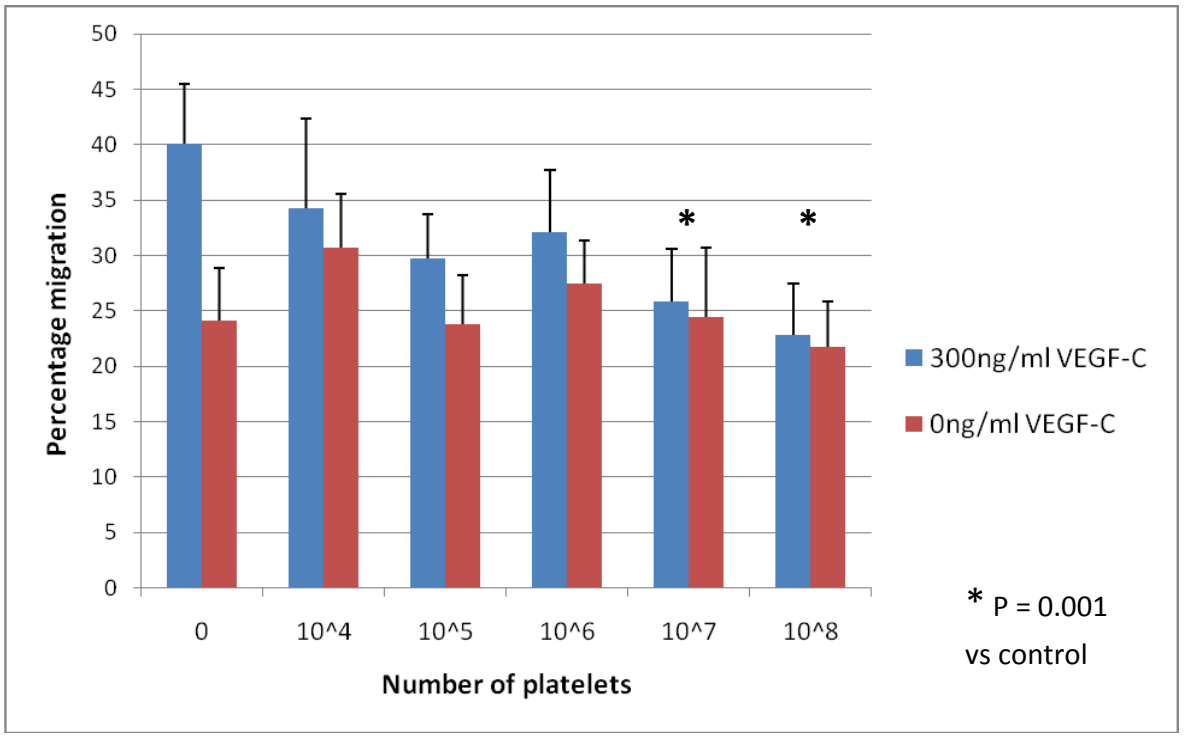

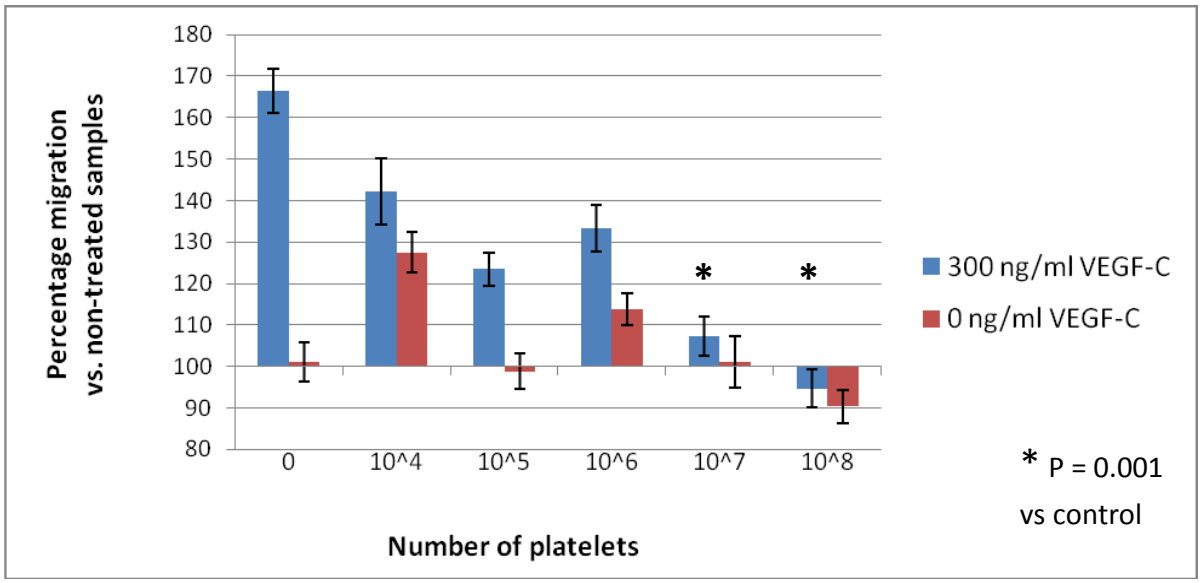

Figure 7: Platelets inhibit VEGF-C mediated migration of HLEC. Cells were applied to the filter and incubated for an hour at 37 °C before the addition of platelets, which were prepared in a volume of 100 µl. The lower chamber of the well contained 300 ng/ml VEGF-C or cell culture medium. (A) Percentage migration of HLEC with the addition of different numbers of platelets. Migration in wells containing 300 ng/ml VEGF-C was inhibited by the addition of platelets (P = 0.001), but the same was not true in wells without VEGF-C. (B) Percentage migration of HLEC plotted as a percentage of the basic level of migration in the absence of VEGF-C and platelets. Error bars on both graphs are the standard deviation of four experiments.

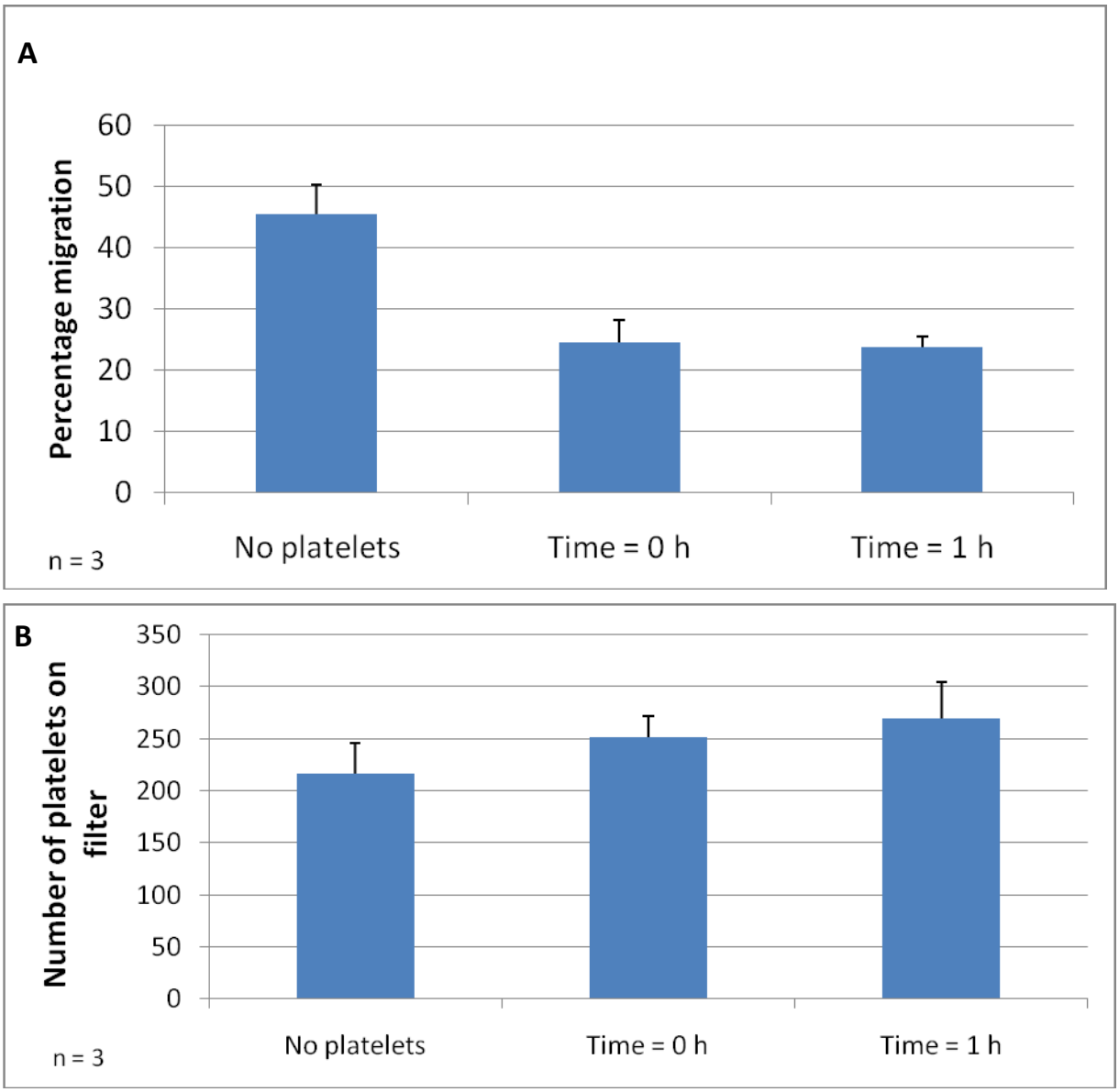

Figure 8: Time of platelet addition does not affect the transmigration assay. The lower chamber of the wells contained 300 ng/ml VEGF-C and HLEC were applied to the filter as in previous experiments. 100 µl of platelets (10^8 cells) was added either immediately after HLEC or an hour later. 100 µl modified Tyrode's buffer was added to the non-treated wells. (A) The different addition times did not affect the level of migration through the filter ($P > 0.05$). (B) There was no significant difference in the average number of cells counted on each filter ($P > 0.05$). Error bars on both graphs represent the standard deviation of three experiments.

3.3. Anti-human podoplanin antibody alone does not inhibit migration

The migration assays above showed that the interaction between platelets and HLEC inhibited the migration of HLEC. The platelet receptor CLEC-2 is known to bind to podoplanin, which is present on the surface of HLEC, so it was hypothesised that this interaction may be responsible for the change in HLEC migration. To test this, an anti-human podoplanin antibody (clone NZ-1.3) was used in the transfilter migration assay. Before this, however, the saturating concentration of the antibody was determined by flow cytometry. HLEC were incubated on ice with concentrations of anti-human podoplanin ranging from 0.15625 μg/ml to 5 μg/ml. The negative controls for this experiment were HLEC with either 2 μg/ml or 20 μg/ml rat IgG. After this first incubation period, 25 μg/ml Alexa 488-conjugated anti-rat was added to each of the tubes, which were incubated on ice for a further 30 minutes. The samples were diluted with PBS before analysis.

Staining with IgG showed similarly low levels of non-specific staining at both 2 μg/ml and 20 μg/ml (Figure 9A & B). As the concentration of anti-human podoplanin antibody was increased, the level of podoplanin staining also increased (Figure 9C). There was little difference between the median fluorescence at 0.625, 2.5 and 5 μg/ml, although there was a slight decrease at 1.25 μg/ml. Therefore, it was decided that the saturating concentration of the antibody was around 2.5 μg/ml and that future experiments would use a concentration of 2 μg/ml. Higher concentrations of antibody were incubated with HLEC to confirm this result and as expected there was no further increase in staining of podoplanin.

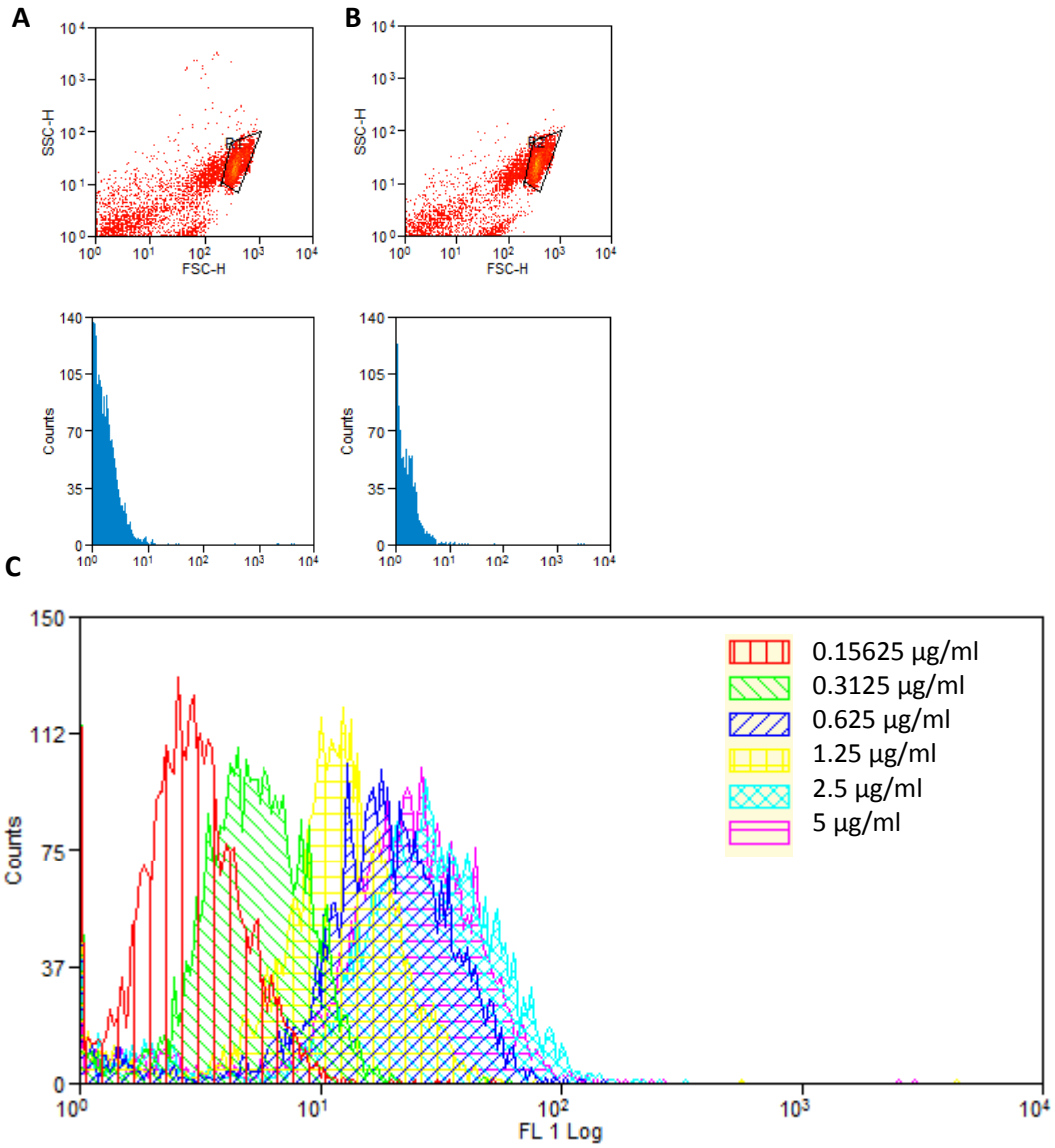

Figure 9: Titration of anti-human podoplanin antibody. HLEC were incubated with varying concentrations of anti-human podoplanin or rat IgG. A gate was applied to intact HLEC prior to analysis. Incubating cells with IgG showed a low level of background staining at (A) 2 µg/ml and (B) 20 µg/ml. (C) Median fluorescence increased with increased concentration of antibody. Fluorescence was similar for antibody concentrations of 0.625, 2.5 and 5 µg/ml, suggesting that saturation was between 0.625 and 2.5 µg/ml.

The anti-human podoplanin antibody used in this study (NZ-1.3) is described in the literature as a blocking antibody that interacts with the podoplanin domains involved in CLEC-2 binding (41). A transmigration assay was performed to determine whether this antibody alone would inhibit VEGF-C mediated HLEC migration and assess if the antibody could abrogate platelet-CLEC-2 binding and alter the effect of platelets on HLEC migration that was seen at 24 hours. Anti-human podoplanin antibody was added 30 minutes after seeding of HLEC and platelets were added after an additional 30 minutes to ensure full HLEC-antibody interaction.

The anti-human podoplanin antibody alone did not prevent HLEC migration (Figure 10), suggesting that podoplanin engagement by monomeric antibody is not sufficient to alter migration. While the migration with rat IgG alone appears lower, this is not statistically significant ($P > 0.05$) and is similar to the level of migration observed in non-treated wells in previous experiments. As expected, platelets inhibited HLEC migration and the combination of rat IgG and platelets produced a similar effect. Interestingly, the antibody only partially inhibited the effect of platelets.

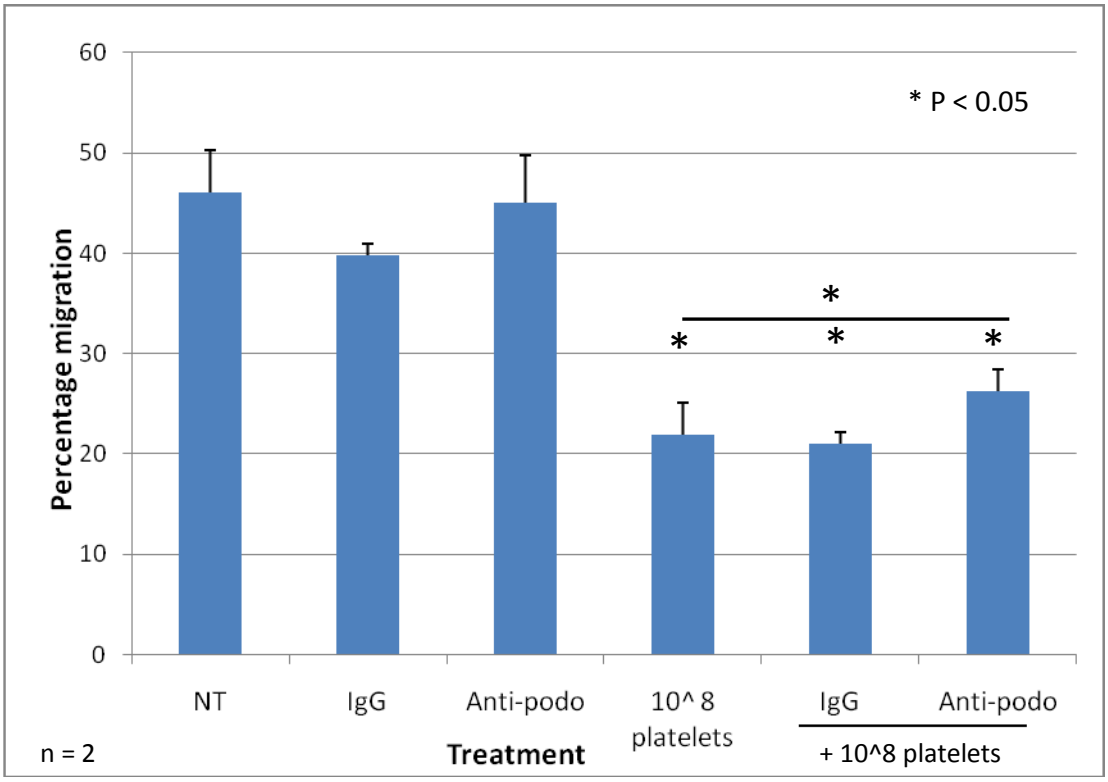

Figure 10: Effect of anti-human podoplanin on HLEC migration. Anti-human podoplanin antibody or rat IgG were added to the filter 30 minutes after HLEC, while platelets were added after a further 30 minutes incubation. The lower chamber of the wells contained 300 ng/ml VEGF-C in cell culture medium. Anti-human podoplanin alone did not alter percentage migration, but partially reversed the effects of platelets ($P < 0.05$). However, there was still a significant inhibition in HLEC migration ($P < 0.05$) compared to the control sample. Error bars are standard deviation of at least two experiments: n = 2 for IgG, anti-podoplanin and IgG + 10^8 platelets; n = 3 for all other conditions.

3.4. Crosslinking of podoplanin reduces the migration of HLEC

The previous experiment showed that anti-human podoplanin binding to HLEC was not enough to alter migration. Given that CLEC-2 is present on the platelet surface as a dimer (Hughes et al., 2010), we hypothesised that further crosslinking of podoplanin may be necessary to induce functional effects.

We assessed the effect of a crosslinking strategy combining the anti-human podoplanin and an anti-rat secondary in the transmigration assay. Initially, different primary:secondary ratios of 1:1, 1:7.5 and 1:15 were tested to determine the optimal assay conditions, keeping the anti-human podoplanin at 2 μg/ml in all cases. The primary to secondary antibody ratio of 1:15 produced a greater inhibitory effect (Figure 11), so was used for the remaining experiments.

As seen in previous experiments, neither anti-podoplanin nor rat IgG alone had any effect on percentage migration (Figure 11). Combining the rat IgG with the anti-rat secondary did not reduce HLEC migration compared to the non-treated control, but, incubating HLEC with both anti-human podoplanin and anti-rat inhibited HLEC migration. This suggests that crosslinking of podoplanin leads to the inhibition of HLEC migration.

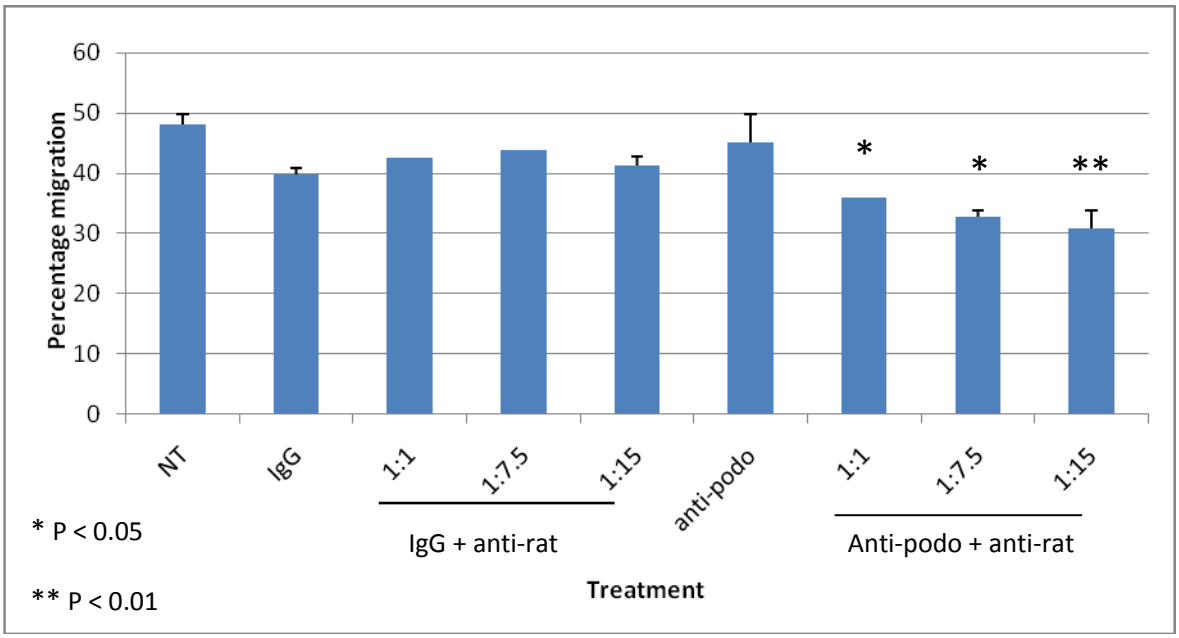

Figure 11: Titration of anti-rat secondary antibody. HLEC were incubated with 2 µg/ml rat IgG or anti-human podoplanin. The anti-rat secondary antibody was added at ratios of 1:1, 1:7.5 and 1:15. Incubation with rat IgG gave similar levels of migration, regardless of the amount of secondary antibody used. In contrast, when anti-human podoplanin was combined with anti-rat, migration decreased. The greatest effect was with a ratio of 1:15 ($P < 0.01$). Error bars, where applicable, represent the standard deviation of two experiments. * $P < 0.05$ and ** $P < 0.001$ vs non-treated HLEC (NT).

We aimed to biochemically confirm that podoplanin is crosslinked by both platelet binding and antibody-mediated methods. HLEC were incubated with either rat IgG or anti-human podoplanin in the absence or presence of the secondary anti-rat IgG, or with washed platelets or fixed platelets before chemical crosslinking with sulfo-EGS. The samples were analysed by SDS-PAGE and anti-podoplanin Western blot. The resulting image showed a band at around 40 kDa, detecting podoplanin (Figure 12). It was anticipated that crosslinked podoplanin would appear as another band of around 80 kDa. However, after antibody-mediated crosslinking the only extra bands detected were those showing the heavy and light chains of the immunoglobulins. Therefore, podoplanin crosslinking could not be proved in this

experiment. Although the platelet-mediated crosslinking did not produce a band that would correspond to crosslinked podoplanin, it gave another band at approximately 50 kDa. This may be associated with podoplanin signalling, but further experiments would be required to confirm this point.

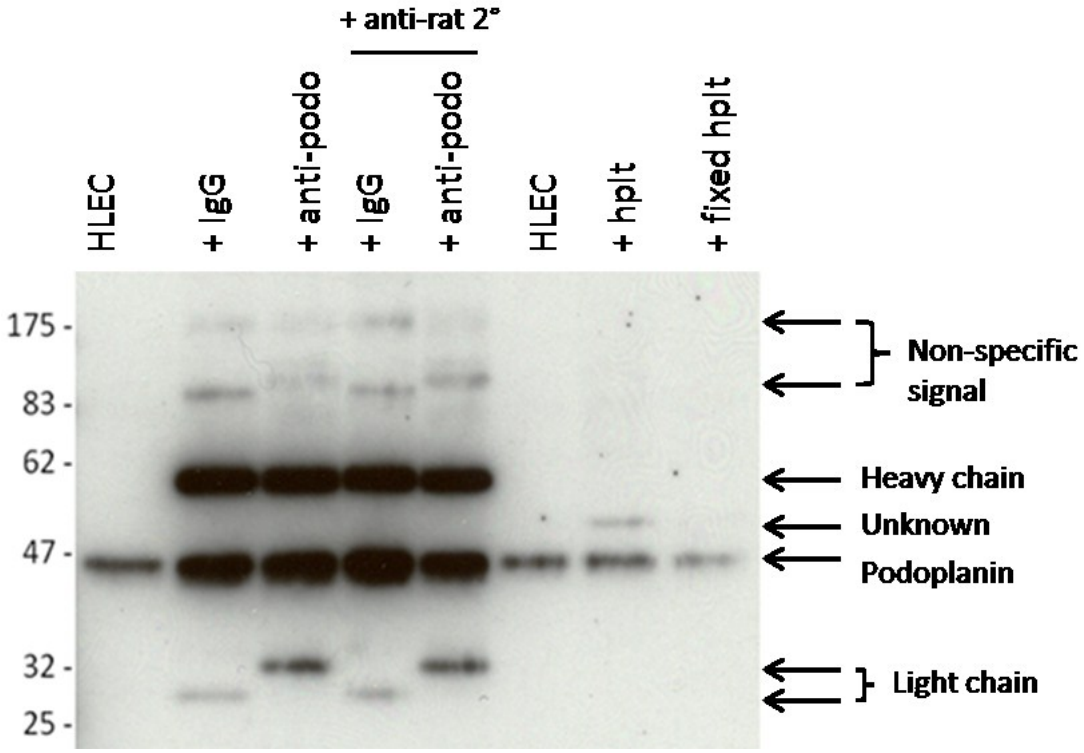

Figure 12: Podoplanin is present in HLEC but cannot be chemically crosslinked by sulfo-EGS. All lanes of the gel showed a band at around 40 kDa, which is podoplanin. The dark band in the samples incubated with anti-human podoplanin or rat IgG (60 kDa) represents the antibody heavy chain, while the bands above are thought to be non-specific signals as they also appeared with the IgG treatment. The antibody light chains are also visible at the bottom of the gel (27 and 32 kDa). The sample that was incubated with washed human platelets has a faint band at 50 kDa. It is not clear what this represents, but it may be associated with podoplanin signalling.

3.5. Crosslinking of podoplanin gives no further inhibition of HLEC migration in the presence of Y27632

Knowing that crosslinking of podoplanin inhibits HLEC migration, we assessed the effect of a Rho kinase inhibitor, Y27632, on HLEC migration. Anti-human podoplanin was applied to the filter 30 minutes after HLEC. This was followed by anti-rat after a further 30 minute incubation. Finally, after HLEC had been incubated with the antibodies, 100 μM Y27632 was added to the filter. The lower chamber of the wells contained 300 ng/ml VEGF-C. The non-treated control contained HLEC with PBS as this the diluent used to prepare both the antibodies and Rho kinase inhibitor. Y27632 inhibited HLEC migration at a level similar to that of the combined anti-podoplanin and anti-rat antibodies (Figure 13). Combining the inhibitor with the antibodies had no additional effect: the decrease in migration was the same as that seen with the antibodies alone.

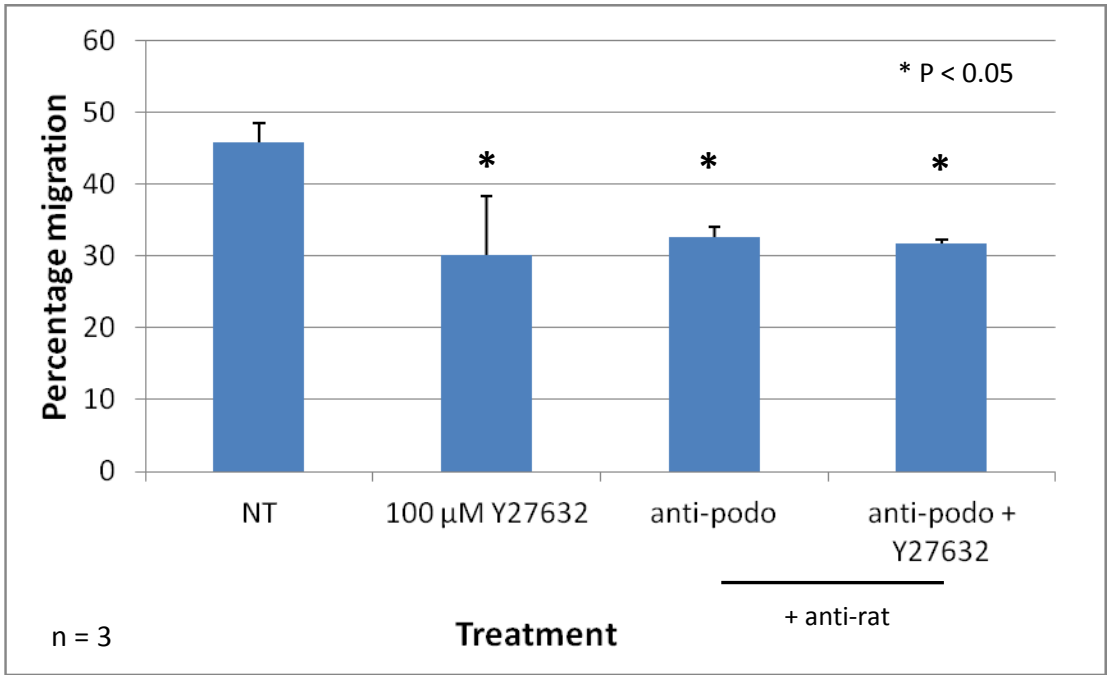

Figure 13: Crosslinking podoplanin does not give any further inhibition of migration in the presence of Y27632. Anti-human podoplanin antibody was added to HLEC and incubated for 30 minutes before the secondary antibody was added. After a further 30 minute incubation, 100 µM of the Rho kinase inhibitor Y27632 was applied to the filter. Y27632 alone inhibited HLEC migration, as did the antibody-mediated crosslinking of podoplanin. However, when the two treatments were combined there was no additive effect. Error bars represent the standard deviation from three experiments. * $P < 0.05$ compared to non-treated control (NT). There was no significant difference between migration with Y27632, crosslinking antibodies or the combination of both treatments.

3.6. Inhibition of Rho kinase reduces platelet-mediated inhibition of migration

Finally, the Rho kinase inhibitor Y27632 was used alongside platelets in the transfilter migration assay. HLEC were applied to the filter and 100 µM Y27632 was added 30 minutes later. After a further 30 minutes, 10^8 platelets were added to the filter. 300 ng/ml VEGF-C was added to the lower chamber of the well as the effect of platelets was found to be specific to VEGF-C mediated migration. As expected, platelets significantly inhibited HLEC migration (Figure 14) and Y27632 also inhibited migration, although to a lesser extent. When the platelets and Rho kinase inhibitor were combined, there was no further inhibition of migration than that seen with Y27632 alone.

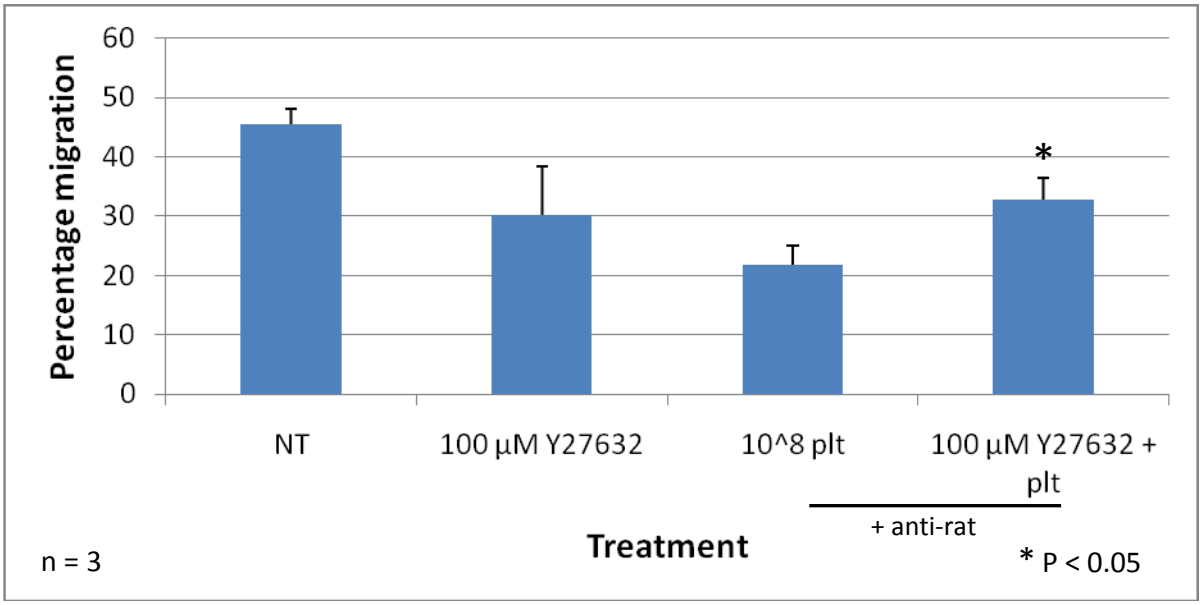

Figure 14: Combining platelets and Y27632 results in a partial recovery of HLEC migration. As in earlier experiments, both the Rho kinase inhibitor Y27632 and platelets inhibit the migration of HLEC, although the data shows that platelets have a more profound effect. When the inhibitor and platelets were combined there was still an inhibition of migration, but it was less pronounced than with platelets alone. Error bars are the standard deviation of three independent experiments. * P < 0.05 compared to 10^8 platelets.

4. DISCUSSION

4.1. Summary of results

The results from this project indicate that the interaction between platelets and HLEC causes a reduction in the migratory potential of HLEC and that this may be through the interaction of podoplanin and CLEC-2. Cell migration assays showed that a high number of platelets inhibit VEGF-C mediated HLEC migration and that adding platelets to the filter immediately after HELC does not have a significant effect. Crosslinking of podoplanin with the NZ-1.3 antibody and an anti-rat secondary also inhibits HLEC migration, while the NZ-1.3 antibody alone does not inhibit migration. The antibody alone partially blocks the effect of platelets. The Rho kinase inhibitor Y27632 nullified the effects of both platelets and crosslinking antibodies on HLEC migration.

4.2. Platelets reduce VEGF-C mediated migration of HLEC

Mice deficient in either podoplanin or CLEC-2 develop a blood-lymphatic mixing phenotype, which is believed to be due to incomplete separation of the blood and lymphatic vessels (21,39). Human platelets are able to inhibit the migration of HLEC and platelets from CLEC-2 knockout mice allow a partial recovery from this effect (Navarro-Núñez et al., unpublished data). The transfilter migration experiments confirmed that a high number of human platelets will inhibit HLEC migration, suggesting that platelets alter HLEC signalling. This alteration in signalling could be through the interaction of podoplanin and CLEC-2, which was examined further in later experiments. These experiments also showed that the effect of platelets was specific to VEGF-C mediated migration. This may be due to an

interaction between podoplanin and VEGF-C signalling pathways within the HLEC, but further experiments would be required to prove this theory.

VEGF-C acts on the VEGFR-3 receptor and is known to promote both migration and proliferation of HLEC (11). It is found in the mesenchyme of areas of lymphatic development (10) and is thought to be essential for lymphangiogenesis. In the transfilter migration assay, the inhibitory effect of platelets was only observed in wells containing VEGF-C. It has been suggested that the platelets in the assay may have been metabolising the VEGF-C. However, this is unlikely as the HLEC were incubated with VEGF-C for an hour before the addition of platelets, meaning there was sufficient time for VEGF-C signalling to occur. In addition to this, when platelets were added to the filter immediately after HLEC the result of the assay was no different and the platelets still inhibited HLEC migration.

This second experiment also proved that platelets were not affecting the viability or adhesion of the HLEC. The average number of cells on each filter was similar regardless of treatment, proving that platelets neither prevent HLEC adhesion nor promote cell death. This also supports the hypothesis that platelets are changing the signalling within HLEC rather than reducing of the number of adherent cells, which could result in a lower percentage migration.

4.3. Anti-human podoplanin antibody alone does not inhibit HLEC migration

Having shown that platelets reduced the migration of HLEC, an anti-human podoplanin antibody was used to determine whether it was the interaction between CLEC-2 and podoplanin that was causing this change in migration. The NZ-1.3 antibody alone had no effect on HLEC migration, indicating that podoplanin ligand engagement is not sufficient to alter signalling. The addition of the same concentration of antibody partially reversed the effect of platelets in this assay, suggesting that the antibody was not entirely blocking the CLEC-2 binding site of podoplanin, allowing platelets to bind and exert their anti-migratory effect. It is possible that platelets were able to bind to HLEC because the antibody used was not truly a blocking antibody as had been stated in the literature (41). Further experiments, including an assessment of CLEC-2 – podoplanin binding would have to be performed in order to confirm this.

4.4. Crosslinking of podoplanin inhibits HLEC migration

Although the transfilter experiments had shown that the NZ-1.3 antibody alone could not inhibit HLEC migration, we assessed whether crosslinking podoplanin may have an inhibitory effect on migration. The assay was characterised by determining the optimal ratio of NZ-1.3 to anti-rat secondary antibody. An antibody ratio of 1:15 was found to have the greatest inhibitory effect. These conditions were then used in an experiment comparing the effect of NZ-1.3 with and without the anti-rat secondary. This confirmed that crosslinking of podoplanin inhibits HLEC migration, although the change in migration was less pronounced

than that seen with platelets. This data suggests that the crosslinking of podoplanin by antibodies alters podoplanin signalling. It is possible that this change in signalling prevents the cytoskeletal rearrangements necessary for migration to occur, but this could not be tested during the project.

We attempted to crosslink podoplanin using antibodies or platelets with sulfo-EGS as the chemical crosslinker, but this experiment did not produce the expected result. This is most probably due to the sulfo-EGS itself, which has a spacer arm distance of 16.1 Å. On reflection, this is probably not wide enough to stabilise crosslinked podoplanin molecules. Although this experiment did not show evidence of podoplanin crosslinking there was a band of unknown origin on the Western blot that could be of interest. This faint band was seen in the sample containing HLEC and washed platelets and is slightly heavier than podoplanin, at approximately 50 kDa. It is possible that this unidentified band is involved in podoplanin signalling, but more experiments would be needed to confirm this. The first experiment that should be performed is to repeat the platelet-mediated crosslinking in the presence of staurosporine. This would inhibit any protein kinases present in the sample and may, therefore, show whether the unknown band is due to podoplanin phosphorylation or the interaction of podoplanin with a small signalling protein.

4.5. Crosslinking of podoplanin gives no further inhibition of HLEC migration in the presence of Y27632

Podoplanin is known to associate with ERM proteins, which connect the actin cytoskeleton to membrane proteins (24). Podoplanin signalling has also been associated with activation of the Rho GTPase family of proteins, which are signalling molecules involved in the cytoskeletal reorganisation that is required for polarised cell migration. Y27632 is an inhibitor of Rho kinase, a downstream effector of RhoA. Y27632 inhibited HLEC migration, but the effect was not as strong as that seen with 10^8 platelets. This shows that Rho kinase does have a role in migration of HLEC. When Y27632 was combined with the crosslinking antibodies the observed migration was the same as that with the 1:15 ratio of antibodies. This lack of any further effect suggests that the effect of the antibody crosslinking strategy specifically blocks podoplanin signalling, leading to Rho kinase activation instead of a non-specific side effect. Although Rho kinase is implicated in HLEC migration, RhoA has several other downstream effectors. Y27632 only targets one of these: Rho kinase. Therefore, it would be sensible to repeat this experiment with an inhibitor that targets RhoA itself, such as C3 transferase and compare the degree of inhibition with that seen with platelets.

4.6. Inhibition of Rho kinase reduces platelet-mediated inhibition of migration

When Y27632 was used in a transfilter assay alongside 10^8 platelets, there was no further inhibition than that demonstrated by Y27632 alone. One potential explanation for this is that platelets may require activation of Rho kinase to allow them to inhibit HLEC migration, but this would need to be confirmed in future experiments.

4.7. Conclusions and future directions

The hypothesis underlying this project was that crosslinking of podoplanin would prevent the migration of HLEC. The specific aims were to assess the effect of (i) platelet-mediated and (ii) antibody-mediated crosslinking on HLEC migration. The data outlined above demonstrates that platelets inhibit VEGF-C mediated HLEC migration. Similarly, the crosslinking antibodies inhibited HLEC migration. Taken together, these results suggests that platelet CLEC-2 crosslinks podoplanin molecules upon binding, which leads to an alteration in signalling within the HLEC. To confirm the requirement for both CLEC-2 and podoplanin, platelets from CLEC-2 knockout mice and lymphatic endothelial cells from podoplanin-deficient mice could be studied.

The data confirms the requirement for VEGF-C in lymphangiogenesis, as HLEC migration was low in the absence of VEGF-C. As the effect of platelets is specific to VEGF-C mediated migration it is possible that podoplanin crosslinking might modify VEGF-C signalling. However, more work would have to be undertaken to determine whether this is the case.

The mechanism underlying the inhibition of migration still needs to be determined. Initial experiments performed as part of this project suggest a role for Rho kinase, although there may be an additional compensatory mechanism. As Rho kinase, which we inhibited with Y27632, is only one effector of RhoA, the transfilter assays could be repeated in the presence of C3 transferase, a Rho inhibitor. The level of Rho activation at various time

points during the assay could also be assessed to confirm that crosslinking is affecting RhoA activation.

In summary, we have shown that crosslinking of podoplanin with platelets or antibodies reduces VEGF-C mediated migration of HLEC and that the effect of platelets is dose-dependent. Although the mechanism is still unclear, data from this project and previously published work (24,28) indicates a role for RhoA in podoplanin signalling.

REGULATION OF THE PLATELET COLLAGEN RECEPTOR GPVI AND ITS SHEDDASE ADAM10 BY TETRASPANIN MEMBRANE MICRODOMAINS

This project is submitted in partial fulfilment of the requirements for the award of the MRes

ABSTRACT

Tetraspanins are transmembrane proteins that are thought to have a number of roles in the organisation of cell surface proteins. The platelet collagen receptor GPVI has been identified as a component of tetraspanin microdomains. Similarly, its sheddase, ADAM10, has been shown to be tetraspanin-associated and previous work has found that ADAM10 is regulated by a specific subgroup of tetraspanins, known as the 8-Cys tetraspanins. Therefore, the aim of this work was to determine whether ADAM10 activation altered its localisation within the tetraspanin microdomain. We also wanted to confirm whether ADAM17 was associated with CD9 and assess whether the megakaryocyte-like HEL cell line would be a suitable model in which to study tetraspanin regulation of GPVI cleavage by ADAM10.

We found that ADAM10 was associated with platelet tetraspanins regardless of its activation state. From our data, ADAM17 does not appear to be associated with CD9 in platelets, but this may be due to low ADAM17 expression on these cells. HEL cells are not a suitable for studying GPVI cleavage and ADAM10 regulation by tetraspanins. Attempts to knockdown ADAM10 with siRNA were not successful and GPVI staining was lower than in platelets.

ACKNOWLEDGEMENTS

Many thanks go to my supervisor, Mike Tomlinson, for his day-to-day support, guidance and encouragement. Your enthusiasm for science and tetraspanins in particular, is inspirational.

Thanks also go to the other members of the Tomlinson group: Elizabeth Haining, for helping me find blood donors and taking samples; Kabir Khan, for providing A549 cells; Rebecca Bailey and Jing Yang, who both helped with the finer points of Western blotting. It has been a pleasure to work with you all.

Finally, thanks once again to my partner, Adam Baggett, and my family: Kevin, Pat and Jamie Langan. Your support and encouragement has been invaluable.

TABLE OF CONTENTS

1. INTRODUCTION

1.1. Tetraspanins

The tetraspanins are a family of cell surface glycoproteins that are found in a number of species, including humans, mice, fruit flies plants and some multicellular fungi. Humans are known to have 33 different tetraspanins, many of which appear to be expressed in most cell types (42). However, the expression of some tetraspanins is restricted to certain cell types, for example CD53 is expressed specifically by leukocytes (42). The exact function of tetraspanins is still being determined, but it is believed that they play a role in several areas, including i) ligand binding of associated proteins; ii) modulation of signalling; iii) modulation of trafficking; and iv) regulation of proteolytic processes (42). Tetraspanins function through interactions with a number of specific partner proteins and as tetraspanins are involved in a range of different processes, the proteins that they associate with are also diverse. The proteins known to associate with tetraspanins can be divided into four groups: integrins and other adhesion molecules; proteins with immunoglobulin domains; ectoenzymes; and intracellular signalling molecules (43,44).

As well as interacting with partner proteins, tetraspanins are also able to interact with each other in what has been termed the “tetraspanin web”, also known as tetraspanin microdomains (45). These complex microdomains consist of clusters of tetraspanins and their partner proteins and are distinct from lipid rafts (46). The formation of microdomains is thought to be the reason behind the discrepancy between data obtained with anti-tetraspanin antibodies and knockout mice. While experiments with anti-tetraspanin antibodies have shown significant effects on cell behaviour and suggested an essential role

for tetraspanins, several of the knockout mice have unexpected phenotypes, although others have striking phenotypes (47). One notable example is the CD9 knockout mouse: CD9 is highly expressed in most cell types, but the only phenotype the knockout displays is a defect in sperm-egg fusion (48). It has been suggested that knocking out a specific tetraspanin does not produce an obvious phenotype because the microdomain remains intact, but antibodies disrupt the partner proteins in the microdomain, so have a more profound effect on cell function (47). Another difficulty in tetraspanin research is that each cell type can have many different tetraspanins, which may function in a compensatory manner if one is mutated or deleted. This has been shown to be the case with CD9 and CD81, which share about 50 % of their sequences. If CD81 is overexpressed in CD9-deficient eggs, then there is a recovery in the defective sperm-egg fusion previously seen with these cells (49). Similarly, CD9/CD81 double knockout mice develop pulmonary emphysema and secretory cell metaplasia (50), which is not seen in either of the single knockout mice.

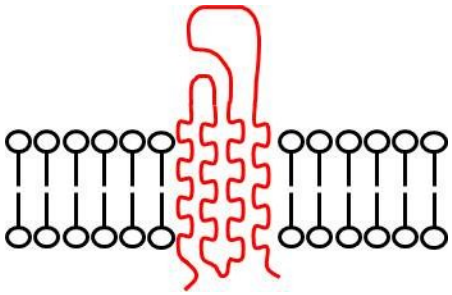

Figure 15: Structure of tetraspanins. Tetraspanins are small cell surface proteins with four transmembrane domains and two extracellular loops. The extracellular domains differ in size, with the second being larger than the first. Tetraspanins can be categorised according to the number of cysteine residues in the large extracellular loop.

Tetraspanins are relatively small proteins and are characterised by four transmembrane domains and two extracellular domains (42), as shown in Figure 15. Both the N- and C-terminals of tetraspanin molecules are cytoplasmic and these cytoplasmic sections of tetraspanins usually consist of less than twenty residues (51). The two extracellular domains differ in size and the structure of the large extracellular loop can be divided into constant and variable regions. The constant region consists of three α-helices, while the variable region contains the majority of the sites that are known to be necessary for interactions with other proteins (52). Tetraspanins also have a number of conserved cysteine residues that are involved in the formation of disulphide bonds and the tetraspanin superfamily can be subcategorised according to the number of cysteine residues present in the large extracellular loop, which can be four, six, seven or eight (52). Of particular interest in this project are those tetraspanins that have eight cysteine residues, known as the "8-Cys" tetraspanins. There are six 8-Cys tetraspanins: Tspan5, Tspan10, Tspan14, Tspan15, Tspan17 and Tspan33. This group of tetraspanins is believed to interact with a disintegrin and metalloproteinase (ADAM) 10 as Tspan33 knockout mice have reduced levels of ADAM10 on their red blood cells (Haining and Tomlinson, unpublished data). While ADAM10 levels on platelets from these mice were normal it is possible that other 8-Cys tetraspanins are able to compensate for the loss of Tspan33 in platelets. In addition to this, the overexpression of 8-Cys tetraspanins has been found to promote trafficking to the plasma membrane and to increase levels of active ADAM10 (Collier and Tomlinson, unpublished data). This association with tetraspanins may have implications for ADAM10's target proteins, including the platelet receptor glycoprotein (GP) VI (53,54).

1.2. Platelets, tetraspanins and GPVI

Platelets play an essential role in haemostasis but also have a role in arterial thrombosis, which can result in myocardial infarction and stroke. Anti-platelet therapies are often used in the treatment of these conditions, but not all patients respond well to these drugs and some develop severe bleeding, which can be fatal. Therefore, understanding how platelet receptors are regulated may reveal new therapeutic strategies for treating myocardial infarction and stroke.

Mice deficient in the platelet tetraspanins CD151 or Tspan32 display a mild bleeding phenotype, which seems to be due to a defect in signalling via $\alpha_{IIb}\beta_3$, the major platelet integrin (55,56). The fact that this phenotype is mild suggests that there are other platelet tetraspanins involved in haemostasis. Initial experiments on the CD9 knockout mouse did not show a platelet phenotype using the standard platelet function tests, such aggregation in the response to various agonists, but intravital microscopy showed that these mice failed to embolise thrombi after ferric chloride injury (57,58). Similarly, CD63 knockout mice displayed a mild platelet phenotype with the only difference detected being a slight *in vitro* hyperaggregation in response to a range of agonists (57,58). In addition to this, Tspan9 knockout platelets have been shown to have a mild defect in spreading and aggregation in response to GPVI-induced activation (Haining and Tomlinson, unpublished data).

Currently, fifteen tetraspanins have been identified on platelets. Most of these proteins are expressed at relatively low levels, with the notable exception of CD9, which is the second most highly expressed protein on the platelet surface (59). Of these fifteen

tetraspanins, the presence of five (CD9, CD63, CD151, Tspan9 and Tspan32) has been confirmed using antibody-mediated methods (60,61). The remaining ten tetraspanins were identified in a proteomics study (59), but these associations have not yet been verified.

The platelet immunoglobulin superfamily protein GPVI has been shown to be associated with tetraspanin microdomains (61). GPVI is a receptor for both collagen and laminin and is specifically expressed by platelets and megakaryocytes. It forms complexes with the Fc receptor γ-chain (FcRγ) via a salt bridge and this complex formation is necessary for GPVI to bind collagen. Through its binding of collagen, GPVI plays an important role in the activation of platelets. After the vascular endothelium has been damaged, platelets are able to transiently adhere to the vessel through the interaction between von Willebrand factor (vWF) and GPIb-IX-V. This allows GPVI to bind to collagen, even though the receptor has a relatively low affinity for collagen. The interaction between GPVI and collagen stimulates an ITAM-mediated signalling cascade that results in the activation of platelets (62).

As GPVI has a role in the activation of platelets and their eventual formation of a thrombus, it has been suggested that targeting GPVI could produce effective anti-platelet therapies. One suggestion has been to reduce the levels of intact GPVI on the platelet surface and one interaction that could be explored further is the action of ADAM10 on GPVI.

1.3. ADAM10 and ADAM17

ADAM10 and ADAM17 are members of the ADAM superfamily of proteins, which are multidomain proteins that have both disintegrin and metalloproteinase domains (63). ADAM proteins have a prodomain that is necessary for correct folding of the immature enzyme (64), but also maintains the protein in an inactive state. In order for the protein to be activated, the prodomain has to be cleaved, which is primarily by furin and PC7 (65).

ADAM proteins function as ectodomain sheddases, cleaving the extracellular region of target proteins. In addition to GPVI, ADAM10 has a number of other important targets, including epidermal growth factor (66), Notch (67) and amyloid precursor protein (68). Defective ADAM10 activity has previously been associated with Alzheimer's disease and cancer (66,69) and may also have a role in inappropriate thrombus formation through its targeting of GPVI. ADAM10 has been shown to be associated with tetraspanins (43,70) and Tspan12 overexpression has been shown to increase levels of mature ADAM10 (71). In addition to the effect of Tspan12 on ADAM10, previous work has also shown that overexpression of the 8-Cys tetraspanins increases the amount of mature ADAM10 (Collier and Tomlinson, unpublished data). It is believed that the association between ADAM10 and 8-Cys tetraspanins is necessary for the trafficking of immature ADAM10 from the endoplasmic reticulum to the cell surface (Figure 16).

The current hypothesis is that when ADAM10 is associated with a tetraspanin it is chaperoned from the endoplasmic reticulum through the Golgi network, where furin and PC7 cleave its prodomain, to its destination at the cell surface. Without the tetraspanin

association, levels of mature ADAM10 at the cell surface are likely to be reduced. In platelets, this would result in more intact GPVI, allowing platelet activation through its binding to collagen. In theory, if surface levels of ADAM10 are reduced then there will be elevated levels of GPVI, potentially allowing excessive platelet activation. However, GPVI cleavage tends to occur when platelets are activated and ADAM10 is not the only protease cleaving GPVI, as it has been shown that ADAM17 and at least one other protease are also able to do this (54). Another complication arises from the possibility that tetraspanins may negatively regulate ADAM10, keeping it inactive whilst at the cell surface to prevent excessive cleavage of GPVI.

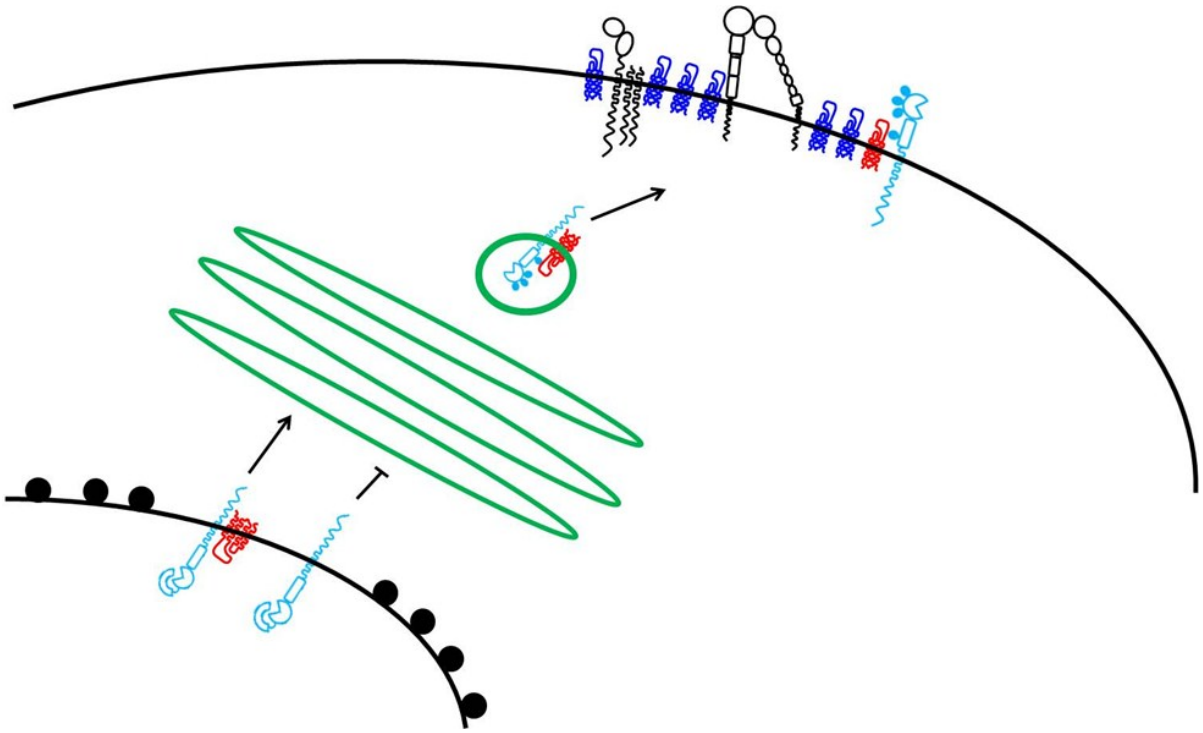

Figure 16: Proposed role of the interaction between ADAM10 and tetraspanins. When associated with tetraspanins, immature ADAM10 is successfully transported through the Golgi to the cell surface, where it becomes associated with the tetraspanin microdomain. Once ADAM10 is within the microdomain, the prodomain is cleaved. However, if ADAM10 does not associate with a tetraspanin, it is unable to be transported from the endoplasmic reticulum, leading to a reduction in mature ADAM10 at the cell surface. Adapted from Haining and Tomlinson, unpublished.

While ADAM10 is known to be tetraspanin-associated, there is currently some debate as to whether ADAM17 is also associated with tetraspanin enriched microdomains. A recent publication has described the association of ADAM17 with CD9 on the surface of both leukocytes and endothelial cells (72), which contradicts previous studies (70,71). Data obtained from knockout mice has shown that ADAM17 is also to cleave GPVI *in vitro* and it is interesting to note that the same study also detected GPVI cleavage in ADAM10/ADAM17 double knockout mice *in vivo*, which suggests that there is at least one other protease acting

on GPVI (54). However, another group claim that ADAM10 is the primary GPVI sheddase and did not show a role for ADAM17 in GPVI cleavage (53).

1.4. Hypothesis and aims of the project

As GPVI is known to be a target of ADAM10 it is possible that through understanding the localisation of these proteins within tetraspanin microdomains a new therapeutic angle for inhibiting platelets will become apparent. It was hypothesised that the localisation of ADAM10 and GPVI within tetraspanin microdomains changes when ADAM10 is activated. Therefore, the aims of this project were:

1. To determine whether activation of ADAM10 and cleavage of GPVI by ADAM10 alters the localisation of these proteins on platelets
2. To confirm whether ADAM17 is associated with CD9 on platelets
3. To assess whether the HEL megakaryocyte-like human erythroleukaemia cell line can be used as a model system for studies involving tetraspanins, ADAM10 and GPVI

2. MATERIALS AND METHODS

2.1. Cell culture

Human erythroleukaemia (HEL) cells were maintained in RPMI medium (PAA, Yeovil, UK) that was supplemented with 10% foetal calf serum, 2 mM L-glutamine and 100 units/ml penicillin and 0.1 mg/ml streptomycin (PAA). These suspension cells were kept at a concentration of 1 x 10^6/ml or less, so were split 1:10 every 3-4 days. A549 cells, a human alveolar epithelial cell line, were maintained in Dulbecco's modified eagle medium (DMEM; PAA) containing 10% foetal calf serum, 1 % L-glutamine and 1 % penicillin-streptomycin. A549 cells were detached for passage or experiments by scraping or using 0.05% trypsin-EDTA (PAA).

2.2. Preparation of washed human platelets

Whole blood was taken from healthy volunteers who had given informed consent and had not taken any medication that would affect platelet function. Blood was drawn into 4% sodium citrate (1:9 volume) and to prevent platelet activation 10% acid citrate dextrose (ACD: 120 mM sodium citrate, 110 mM glucose and 80 mM citric acid) was added to the blood. The blood was centrifuged at 200 xg for 20 minutes. 10 µg/ml prostacyclin was added and the sample was centrifuged for 10 minutes at 1000 xg. The pellet was resuspended in warm modified Tyrode's buffer (134 mM NaCl, 2.9 mM KCl, 0.34 mM Na_2HPO_4, 12 mM $NaHCO_3$, 20 mM HEPES, 1 mM $MgCl_2$; pH 7.3) containing 5 mM glucose. A further 24 ml Tyrode's was added with 3 ml ACD and 10 µg/ml prostacyclin. The platelets

were centrifuged for a further 10 minutes at 1000 xg. The pellet was resuspended in 5 ml modified Tyrode's buffer and counted using a cell counter (Coulter, High Wycombe, UK).

2.3. Flow Cytometry

2.3.1. Platelets

Flow cytometry was used to assess whether W7 (Calbiochem, Nottingham, UK) and N-ethyl maleimide (NEM; Calbiochem) were activating ADAM10, which would be demonstrated by a decrease in intact GPVI. 1 x 10^8 washed human platelets were incubated for an hour at 37 °C with 2 mM NEM, 150 µM W7 or DMSO in a final volume of 1 ml. 5 µl of each treatment was transferred to FACS tubes and incubated with 10 µg/ml anti-human CD9 (clone 1AA2, gift from Prof Leonie Ashman), anti-human GPVI (clone: 204-11; gift from Prof Masaaki Moroi) or negative control MOPC IgG monoclonal antibody (Sigma, Poole, UK) for 30 minutes at room temperature. 1 mM EGTA in Tyrode's buffer was added to each tube and unbound antibody removed by centrifuging at 1000 x g for 5 minutes. Anti-mouse IgG-FITC was then incubated with the platelets for 30 minutes. Samples were diluted with 500 µl FACS buffer (0.2 % bovine serum albumin and 0.02 % NaN_3 in PBS) before analysis on a FACSCalibur flow cytometer (BD Bioscience, Oxford, UK) using Cellquest. A gate was applied around intact cells and data collected from 10,000 events.

2.3.2. HEL cells

1 x 10^6 HEL cells were incubated at 37 °C for an hour with 1 mM NEM, 150 µM W7 or the vehicle controls (ethanol or DMSO). Each sample was divided between FACS tubes and indirect staining using MOPC or GPVI (204-11) antibodies, followed by an anti-mouse IgG secondary, was performed. Samples were diluted with 500 µl FACS buffer containing 2 µg/ml propidium iodide (Sigma) before analysis. A gate was applied around live cells and data was collected from 5,000 events.

Analysis of ADAM10 knockdown in HEL cells was by flow cytometry. An indirect staining approach for MOPC, CD9 (1AA2) and ADAM10 (clone 163003, R&D Systems, Abingdon, UK) was used. The secondary antibody was the same as in the previous experiments. The samples were diluted in 500 µl FACS buffer and analysed as above.

In later experiments assessing ADAM10 knockdown, a direct staining approach was used to stain cells for ADAM10. The FITC-conjugated ADAM10 and isotype control antibodies (R&D Biosystems) were used at a concentration of 1.25 µg/ml and FACS analysis was as described above.

2.3.3. A549 cells

A549 cells were used as a positive control in the siRNA-mediated ADAM10 knockdown experiments. 1.5 x 10^5 cells were stained for MOPC or ADAM10 (163003). Initially this was using an indirect approach, but in later experiments

directly conjugated antibodies were available, so a direct staining approach was used. The cells were diluted in FACS buffer with 2 µg/ml propidium iodide before being analysed on the FACSCalibur.

2.4. Biotinylation and immunoprecipitation of human platelets

Initial experiments assessed the effect of ADAM10 activation by W7 on the localisation of ADAM10 and GPVI. 50 µl protein G sepharose beads (Invitrogen, Paisley, UK) were combined with 2.5 µg of MOPC, anti-human ADAM10 (163003), anti-human CD9 (1AA2) or anti-human GPVI (204-11). The beads were incubated overnight at 4 °C on a rotator.

Washed human platelets resuspended in a volume of 2.5 ml Tyrode's buffer (with 2 mM $CaCl_2$) and were incubated with DMSO or 150 µM W7 for an hour at 37 °C. Platelets were treated with 1 mg/ml sulfo-NHS-LC-biotin (Thermo Scientific, Loughborough, UK) and incubated for 30 minutes at room temperature before the reaction was quenched with 125 mM glycine. The platelets were pelleted and resuspended in 2.5 ml PBS before being divided between five 1.5 ml tubes and lysed with an equal volume of 2x Brij 97 lysis buffer (2 % Brij97, 20 mM Tris at pH 7.5, 150 mM NaCl, 2 mM $CaCl_2$, 2 mM $MgCl_2$, 0.02 % NaN_3) containing 1:100 protease inhibitor cocktail (P8340; Sigma). 20 µl protein G sepharose was added to each tube, which were rotated at 4 °C for 60 minutes to pre-clear the lysates.

The debris was pelleted and the supernatants pooled. 50 µl of each supernatant was added an equal volume of 2x non-reducing sample buffer. The

rest was divided between tubes containing the antibody-coupled beads, which had been washed in Triton X-100 lysis buffer. The samples were then incubated for a further 75 minutes at 4 °C. After this incubation the samples were washed four times with ice-cold Triton X-100 lysis buffer before being transferred to a clean 1.5 ml tube. All lysis buffer was aspirated before 50 µl 2x non-reducing sample buffer was added to each tube. The samples were stored at - 20 °C and analysed by SDS-PAGE and Western blotting at a later date. This experiment was repeated with a slight change in the incubation conditions: the platelets were resuspended in Tyrode's buffer and 2 mM $CaCl_2$ was then added to the W7-treated sample only.

In later experiments we assessed whether ADAM17 was associated with CD9. The protein G sepharose beads were coupled to 2.5 µg MOPC, anti-human ADAM10 (163003), anti-human ADAM17 (clone 111633; R&D Systems) or anti-human CD9 (1AA2). The platelets were biotinylated as before, but half were lysed in 2x Brij97 with the remainder lysed in 2x Triton X-100. The immunoprecipitations were performed as described above, but the washes used either Brij97 or Triton X-100, depending on which buffer the cells had been lysed in. After washing, 50 µl 2x non-reducing sample buffer was added to each tube. The samples were kept at -20 °C until analysis by Western blot at a later date.

2.5. SDS-PAGE and Western blot

Proteins were resolved using a 4-12% gradient gel (NuPAGE, Paisley, UK) under non-reducing conditions. Samples were boiled for 5 minutes and centrifuged briefly before being loaded onto the gel. 2.5 µl molecular weight biomarker (New England Biolabs, Hitchin, UK) in 17.5 µl 2x non-reducing sample buffer was loaded into the first lane of the gel and 1 µl biomarker in 19 µl buffer was put in the last lane. All empty lanes contained 20 µl non-reducing sample buffer. The tank was filled with running buffer (50 mM MOPS, 50 mM Tris base, 0.1% SDS and 1 mM EDTA; NuPAGE) and run at 125 V for approximately 2 hours.

The gel was removed and soaked in transfer buffer (25 mM Tris, 190 mM glycine, 20% methanol) for 30 minutes, while the PVDF Immobilon FL membrane (Millipore, Watford, UK) was wetted with methanol before being soaked in transfer buffer. The transfer chamber was set up with the gel and membrane sandwiched between pre-soaked filters and foam pads. The transfer was run at 30 V for 90 minutes. After transfer, the membrane was blocked with TBS (20 mM Tris, 137 mM NaCl, pH 7.6) containing 3 % bovine serum albumin (BSA) and 0.1 % sodium azide for an hour at room temperature. The primary antibody, either anti-human CD9 or anti-human ADAM10, was prepared in 10 ml of TBS-T (20 mM Tris, 137 mM NaCl, 0.1 % Tween, pH 7.6) containing 3 % BSA and 0.1 % sodium azide. The membrane was incubated with the antibody overnight at 4 °C.

The membrane was washed three times in high salt TBS-T (20 mM Tris, 500 mM NaCl, 0.1 % Tween) for 10 minutes. The secondary antibodies, anti-mouse 680 (Li-Cor, Cambridge, UK) with or without neutravidin (Perbio, Cramlington, UK), were prepared at a 1/10,000 dilution in TBS-T containing 3 % BSA and 0.1 % sodium azide. The membrane was incubated with this solution for 90 minutes at room temperature before being washed for 5 x 5 minutes with high salt TBS-T. A final wash with TBS was then performed. The membrane was blotted dry and analysed using an Odyssey infrared imaging system (Li-Cor).

2.6. siRNA knockdown of ADAM10

8×10^5 HEL cells and 1.5×10^5 A549 cells were applied to 6-well plates in a volume of 2 ml antibiotic-free medium. To make the HEL cells adherent and thus potentially more amenable to transfection, they were treated with 6.2 ng/ml phorbol 12-myristate 13-acetate (PMA; Calbiochem) for 24 hours. 2.5 µl of 4 µM control or ADAM10 siRNA (ID 1005; Applied Biosystems, Warrington, UK) was mixed with 167.5 µl Optimem (GIBCO, Paisley, UK) and separately, 7.5 µl RNAiMAX (Invitrogen) was added to 67.5 µl Optimem. Both solutions were then incubated at room temperature for 10 minutes, after which 30 µl of RNAiMAX solution was added to each siRNA preparation. After incubating for a further 10 minutes, 200 µl siRNA-RNAiMAX solution was added to the cells, giving a final siRNA concentration of 10 nM. The cells were incubated with this solution for four hours at 37 °C before it was replaced with antibiotic-free medium. After incubating at 37 °C for 72 hours, the cells were detached using 0.05 % trypsin-EDTA, transferred to FACS tubes and

indirectly stained for MOPC or ADAM10 before being analysed by flow cytometry. When this experiment was repeated a direct staining approach was used. FITC-conjugated anti-human ADAM10 antibody (R&D Systems) was used and a FITC-conjugated isotype-matched mouse IgG (R&D Systems) was used as the control. As before, analysis was by flow cytometry.

Finally, a time course experiment was performed. 2 x 10^6 HEL cells were treated with 6.2 ng/ml PMA before being transfected with control or ADAM10 siRNA as before. The cells were then incubated for 48, 72 or 96 hours before being analysed by flow cytometry using a direct staining approach.

3. RESULTS

3.1.W7 and NEM induce GPVI shedding in platelets

W7 and NEM are both believed to activate ADAM10 and thus induce GPVI shedding from the platelet surface (53,54). The pro-domain of ADAM10 contains a cysteine switch, which consists of a thiol that inhibits metalloproteinase activity. This thiol is modified by NEM, resulting in restoration of ADAM10's metalloproteinase activity. Ectodomain shedding by ADAMs is also regulated by calmodulin, which is associated with the cytoplasmic domain of GPVI (73). W7, a calmodulin inhibitor, is thought promote GPVI shedding by inhibiting the association between calmodulin and GPVI. This has been shown to be dependent on ADAM10 (54).

To establish a GPVI shedding assay in our lab, we assessed the effect of these drugs on human platelets by comparing GPVI levels in platelet rich plasma (PRP) and washed platelets that had been treated with 150 μM W7, 2 mM NEM or a vehicle control. After the samples had been incubated with the appropriate treatment for an hour, indirect staining for GPVI and the positive control CD9, for which there is no evidence of shedding, was performed before the samples were analysed by flow cytometry. Gating around intact cells showed that incubating platelets with either W7 or NEM resulted in an almost complete loss of GPVI from the cell surface (Figure 17). There was also a reduction in GPVI staining in the washed platelets that had been incubated with the vehicle control, which results from the formation of a secondary shoulder peak on the FACS plot. This may have been due to the presence

of calcium, which was chelated during platelet preparation to reduce the possibility of platelet activation, but was added back to allow ADAM10 to function. There also appeared to be a mild increase in CD9 staining in samples treated with NEM or W7, which is more apparent when the median fluorescent intensities are expressed as a percentage of the staining in the PRP sample (Figure 18). In this experiment, NEM gave a 25 % increase in CD9 compared to PRP, while W7 gave a 50 % increase in CD9 staining (Table 2). In an earlier experiment, which did not include PRP, W7 more than doubled CD9 staining compared to washed platelets treated with DMSO. In this particular experiment, NEM did not appear to increase CD9 staining. This suggests that one consequence of metalloprotease activation might be to render the small non-cleaved CD9 more accessible to antibody staining, due to the shedding of larger proteins that might normally reduce access of the relatively large antibody molecule.

Treatment – experiment 1	**Percentage staining vs washed platelets**
2 mM NEM	93 %
150 μM W7	278 %
Treatment – experiment 2	**Percentage staining vs washed platelets**
2 mM NEM	125 %
150 μM W7	154 %

Table 2: W7 and NEM treatment increase CD9 staining in human platelets. Median fluorescent intensities were normalised before being expressed as a percentage in CD9 staining in the PRP or washed platelet controls. In both experiments, W7 increased CD9 staining, while NEM only increased CD9 staining in the second experiment.

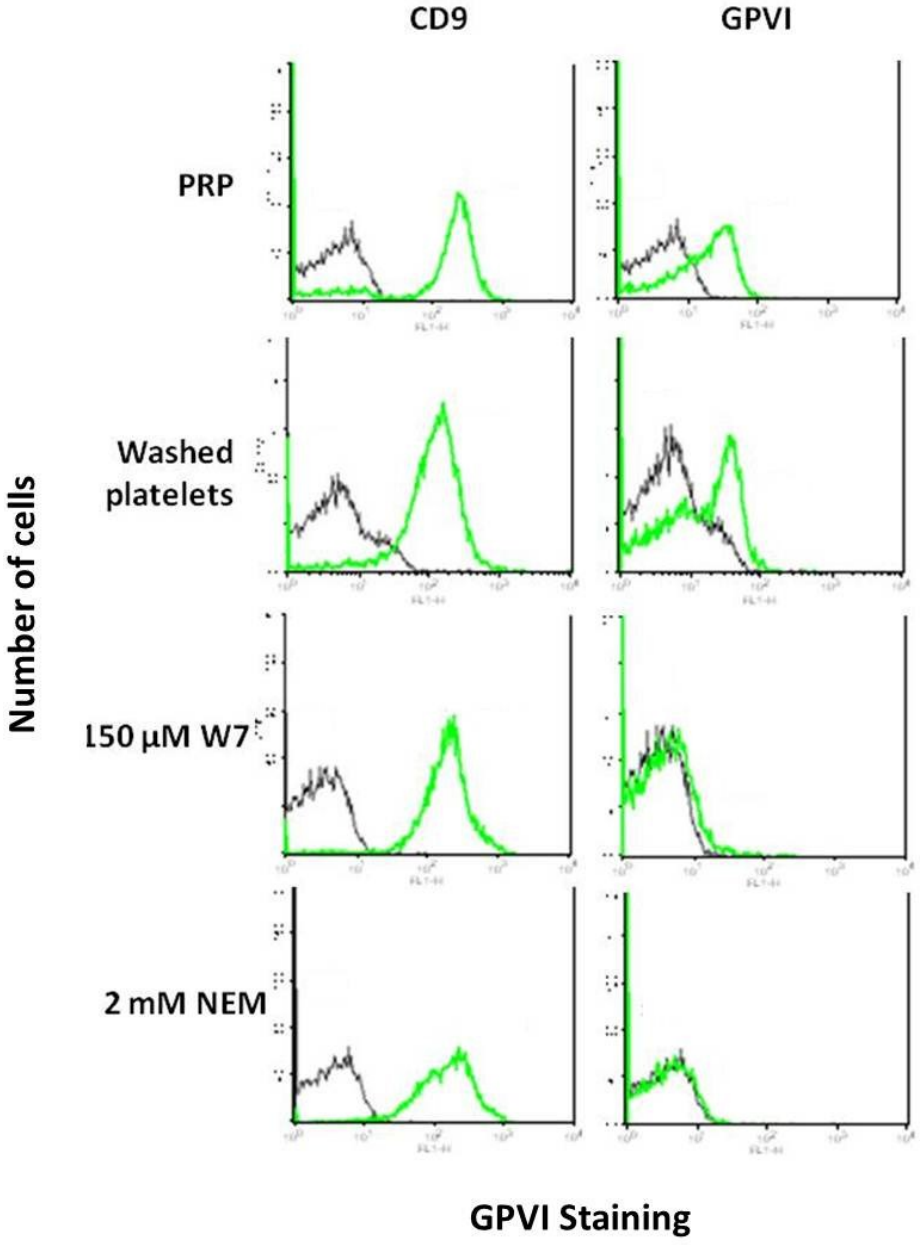

Figure 17: W7 and NEM reduce GPVI levels on platelets. Washed platelets were incubated with 150 µM W7, 2 mM NEM or a vehicle control for an hour at 37 °C. Indirect FACS staining for CD9, GPVI and an irrelevant control (MOPC) was then performed. Both the PRP and vehicle samples showed GPVI staining, which was lost after treatment with W7 or NEM. The washed platelets also showed a shoulder peak, which is thought to be due to calcium in the Tyrode's buffer. While CD9 was used as a positive control, the drugs appeared to increase CD9 staining. N = 1 for PRP and n = 2 for all other samples, traces are representative of both experiments.

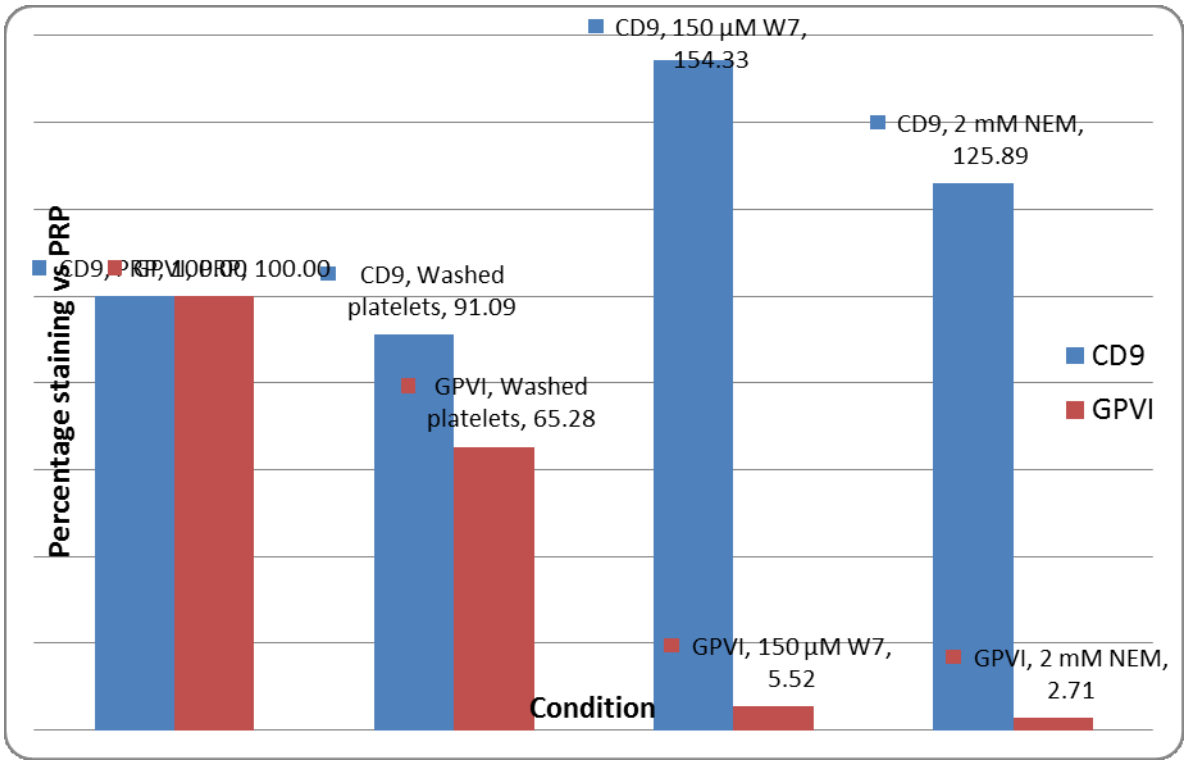

Figure 18: Quantification of CD9 and GPVI staining in human platelets. The median fluorescence intensity was determined in all samples. This was then normalised using the control staining in each sample before being expressed as a percentage of the CD9 or GPVI staining seen in the PRP. The washed platelets that had been incubated with the vehicle showed a 35% decrease in GPVI staining compared to PRP, while there was a 95% decrease after W7 treatment and a 98% decrease after treatment with NEM. In contrast, the CD9 staining increased after treatment with W7 or NEM (by 50% and 25%, respectively). n = 1

3.2.ADAM10 association with tetraspanin microdomains does not appear to be affected by its activation

ADAM10 is known to associate with tetraspanins (43) and it is possible that tetraspanins keep it in an inactive conformation. It was hypothesised that when ADAM10 is activated it is released from the tetraspanin microdomain, allowing it to cleave GPVI. Washed human platelets were incubated for an hour at 37 °C with DMSO or 150 µM W7, which had previously been shown to increase GPVI cleavage. Platelets were then surface biotinylated and immunoprecipitations (IPs) for ADAM10,

CD9, GPVI and a control were performed. The samples were analysed by SDS-PAGE and Western blots with neutravidin (which detects biotin), or antibodies against CD9 and ADAM10.

These biochemical experiments showed that ADAM10 was associated with tetraspanins in both its active and inactive forms. This was apparent in both the neutravidin (Figure 19A) and CD9 (Figure 19B) Western blots. The neutravidin blot showed a pattern of bands in both the ADAM10 and CD9 IPs, which is characteristic of tetraspanins and their associated proteins. The bands in the W7-treated samples appeared darker than in the DMSO samples and we suspected a discrepancy in protein concentration. However, a commercially available protein assay (DC protein assay, BioRad, Hemel Hempstead, UK) confirmed that there was an equal amount of protein in the samples (data not shown). This suggests that W7 treatment makes platelets more amenable to surface biotinylation. In the CD9 blot there was a dark band at approximately 25 kDa, which represents CD9. This was visible in both the CD9 and ADAM10 IPs, confirming that ADAM10 is associated with CD9 in platelets. These samples were also analysed by ADAM10 Western blot (Figure 19C), which showed a band at 70 kDa in both the ADAM10 and CD9 IPs. This band represents ADAM10, therefore confirming the association between these two proteins.

A

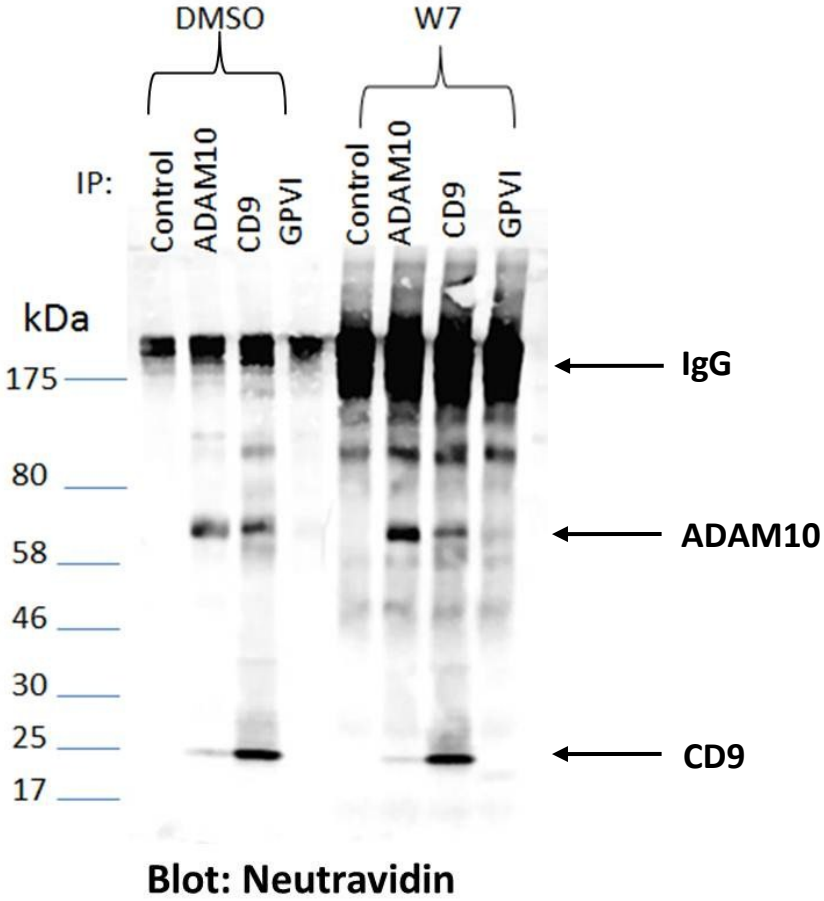
DMSO
W7
IP:
Control
ADAM10
CD9
GPVI
Control
ADAM10
CD9
GPVI
kDa
175
80
58
46
30
25
17
IgG
ADAM10
CD9
Blot: Neutravidin

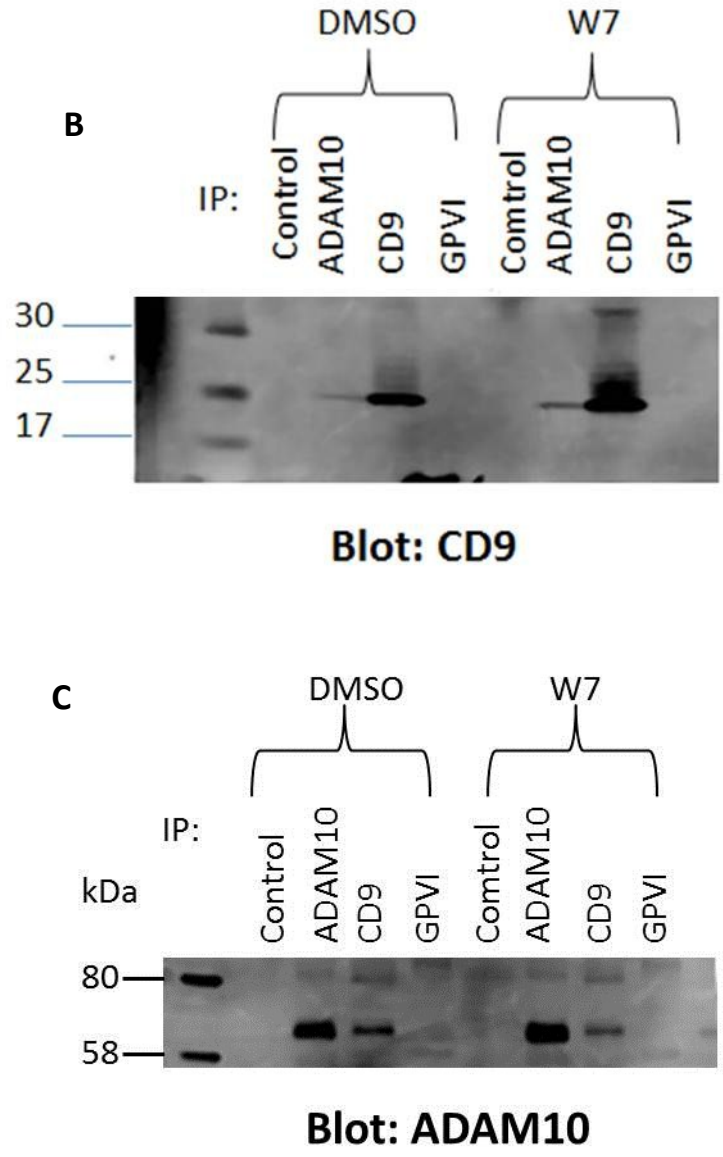

Figure 19: ADAM10 and CD9 are associated in human platelets. Washed human platelets were incubated with either DMSO or 150 µM W7 before being biotinylated. Immunoprecipitations for ADAM10, CD9, GPVI and a control were then performed. (A) The neutravidin blot showed similar band patterns in the ADAM10 and CD9 IPs regardless of treatment. This band pattern is characteristic of tetraspanins and their associated proteins. (B) The 25 kDa band in the CD9 blot represents CD9. This band can be detected in CD9 and ADAM10 IPs from platelets treated with DMSO or W7. (C) The ADAM10 blot showed a band at approximately 70 kDa in the CD9 and ADAM10 IPs. This represents ADAM10 in the samples and treatment with W7 gave the same result as incubation with DMSO. Neutravidin and CD9 blots are representative of three separate experiments.

These biochemical experiments had 2 mM $CaCl_2$ in the Tyrode's buffer that the platelets were resuspended in, but it was later determined that the presence of calcium may have been inducing ADAM10 activation and some cleavage of GPVI in the control samples, which was confirmed by flow cytometry (Figure 17). Therefore, it is important to note that ADAM10 may have been active in the DMSO control, so it is difficult to draw conclusions from this data. To overcome this problem, the experiments were repeated with $CaCl_2$ added to the W7-treated samples only. The neutravidin blots from these experiments also showed that ADAM10 is inactive ADAM10 is associated with tetraspanins (Figure 20).

None of these blots showed the association between CD9 and GPVI, which has been demonstrated previously in this lab (61). This is believed to be due to developing the blots using an infra-red imaging system rather than chemiluminecence. The platelet number used here is also lower than in the Protty study.

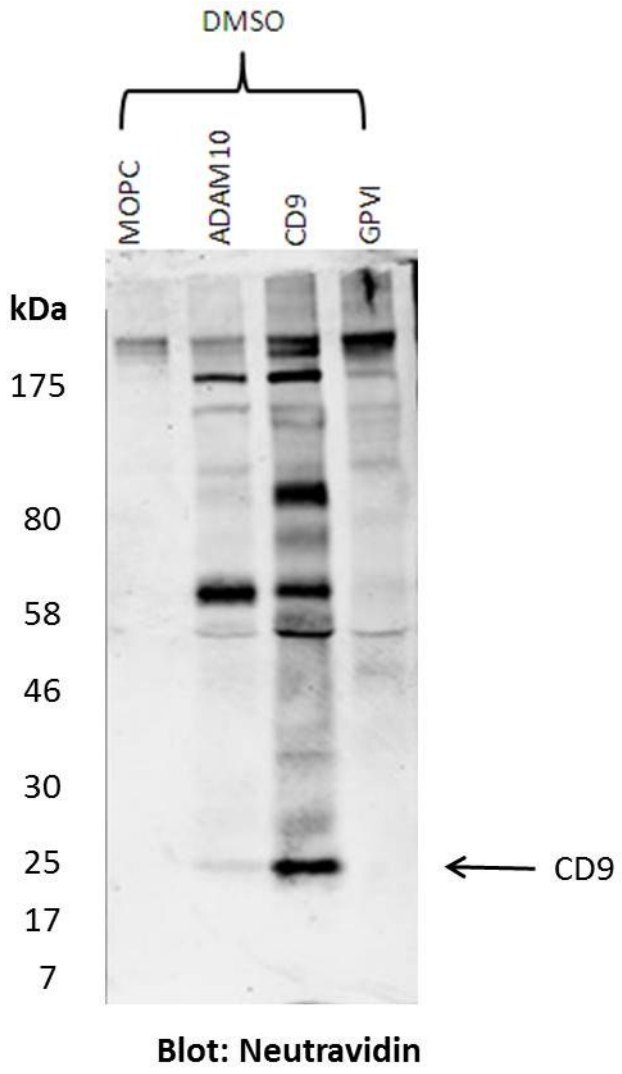

Figure 20: ADAM10 is associated with tetraspanins when in its inactive state. Platelets were incubated with DMSO without $CaCl_2$, before being biotinylated. Immunoprecipitations for ADAM10, CD9, GPVI and a control were then performed. The neutravidin blot showed the same band pattern as that observed in the earlier experiments where the DMSO control contained $CaCl_2$, thus confirming that inactive ADAM10 is associated with tetraspanin microdomains.

3.3.ADAM17 does not appear to be associated with CD9 in platelets

There is currently some debate as to whether ADAM17 is associated with the tetraspanin CD9. A recent paper has shown the association in both leukocytes and endothelial cells (72), but this contradicts previous studies that claimed there was no association between ADAM17 and CD9 (70,71). In addition to this, proteomics studies have found ADAM10 sequences associated with tetraspanins, but not ADAM17 sequences (74). It is, however, possible that this association was not detected as ADAM17 levels were too low on the cells used for the study. As CD9 is relatively abundant on platelets, we examined whether ADAM17 is associated with CD9 in platelets. Washed human platelets were biotinylated and control, ADAM10, ADAM17 and CD9 IPs were performed in both Brij97 and Triton X-100 lysis buffers. The samples were analysed by SDS-PAGE and neutravidin Western blot.

The neutravidin blot showed similar band patterns in the ADAM10 and CD9 IPs that were performed in Brij97 lysis buffer (Figure 21A), consistent with the localisation of these molecules to tetraspanin microdomains on platelets. In contrast, the ADAM17 IP did not show the same band pattern, suggesting that it is not associated with CD9 in platelets. When the exposure on the blot was increased, a band at approximately 130 kDa became visible (Figure 21B). This could be ADAM17, based on its expected molecular weight. However, it is possible that ADAM17 was not immunoprecipitated in this experiment, either because the expression level is low compared to ADAM10 or due to a failure of the ADAM17 antibody to effectively

bind ADAM17. Therefore, this preliminary experiment should be repeated in future with a positive control ADAM17 lysate. The samples that had been prepared in Triton X-100 did not have the same band pattern as this stronger detergent severed the interactions between the different proteins in the tetraspanin microdomain. Therefore, only the primary protein, ADAM10 or CD9, was visible.

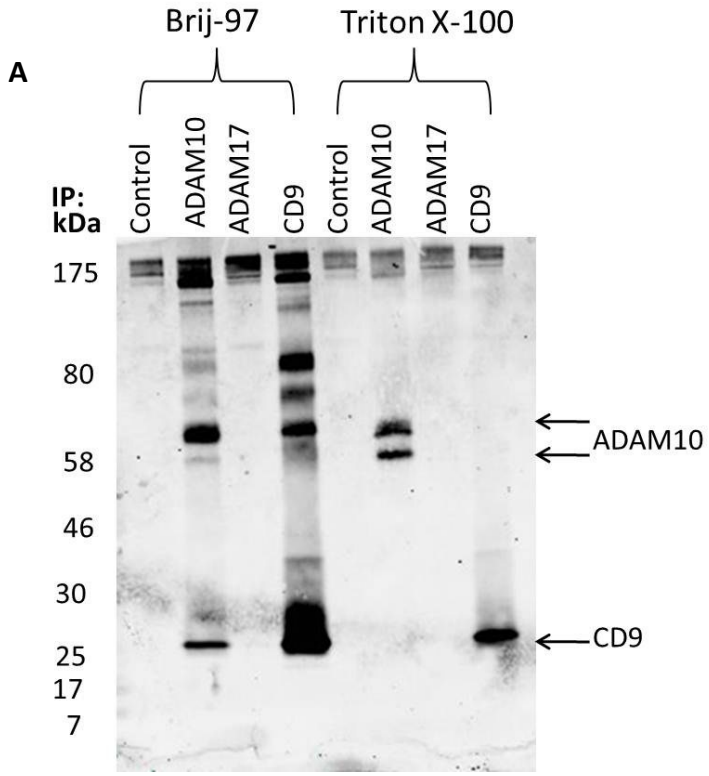

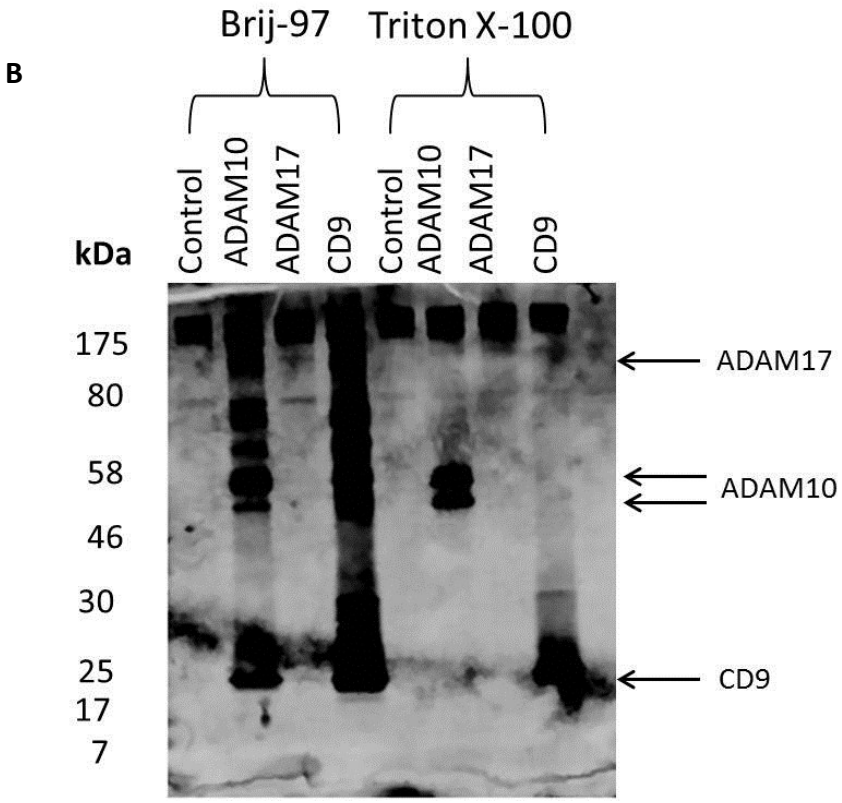

Figure 21: ADAM17 does not appear to be associated with CD9 in human platelets. Human platelets were biotinylated and immunoprecipitations for ADAM10, ADAM17, CD9 and an irrelevant control were performed in both Brij97 and Triton X-100 lysis buffers. The samples were analysed by SDS-PAGE and neutravidin Western blot. (A) Both the ADAM10 and CD9 IPs prepared in Brij97 showed a band pattern that is characteristic of tetraspanins, confirming that ADAM10 is tetraspanin-associated. The same was not true of ADAM17, suggesting it is not associated with tetraspanins. (B) The ADAM17 IP performed in Brij97 showed a single band at 130 kDa, which is believed to be ADAM17. Blots are representative of two separate experiments.

3.4.W7 and NEM induce GPVI cleavage in HEL cells

Another aim of this project was to assess whether the HEL cell line would be a suitable model for studying ADAM10 and GPVI. Since human platelets are not amenable to genetic modification, such a cell line model would allow ADAM10 cleavage of GPVI to be studied in the context of a tetraspanin siRNA knockdown or

overexpression. The first stage in this assessment was to ensure that W7 and NEM were activating ADAM10, as shown by a decrease in intact GPVI. As with the equivalent experiment in platelets, this was done by incubating the cells at 37 °C for an hour with the appropriate drug or a vehicle control and determining GPVI levels by flow cytometry.

The flow cytometry data showed that both 150 µM W7 and 2 mM NEM lowered GPVI levels in HEL cells (Figure 22), although GPVI staining intensity was low compared to that on platelets (Figure 17), suggesting that HEL cells are not an ideal model in which to study GPVI. The median fluorescent intensities were normalised before being expressed as a percentage of the GPVI staining in the control sample. This quantification showed that 2 mM NEM gave an 80% reduction in GPVI staining and 150 µM W7 gave a 40% decrease, suggesting that in this experiment NEM was more effective than W7 at activating ADAM10, as shown by the reduction in intact GPVI.

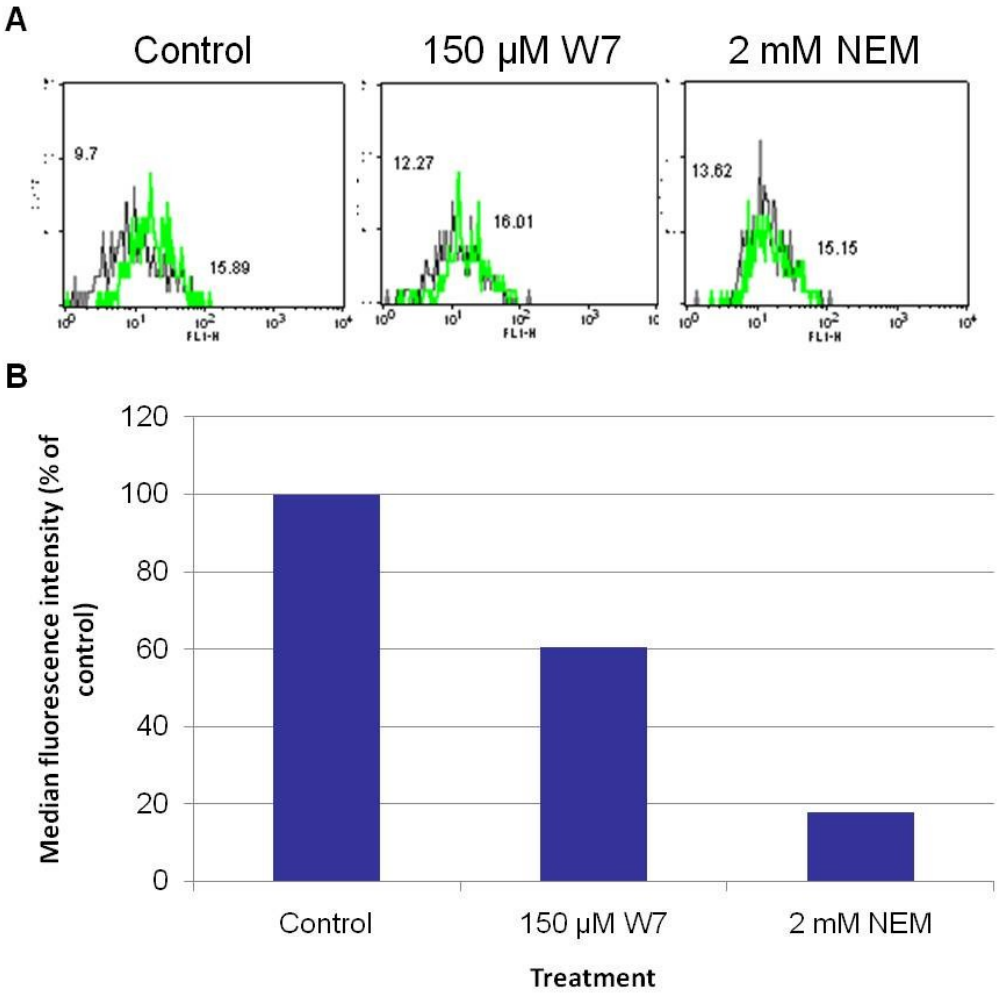

Figure 22: W7 and NEM induce GPVI cleavage in HEL cells. HEL cells were treated with 150 µM W7, 2 mM NEM or a vehicle control for an hour at 37 °C. The cells were then stained for GPVI and an irrelevant control using an indirect method. (A) Flow cytometry data showed a slight shift in the GPVI peak in both the W7- and NEM-treated samples. (B) When the FACS data was quantified using the median fluorescence intensity W7 was shown to reduce GPVI by 40%, while NEM reduced GPVI by approximately 80% (compared to the control sample).

3.5.siRNA-mediated knockdown of ADAM10 is not effective in HEL cells

Having shown that W7 and NEM could activate ADAM10 in HEL cells we attempted to knockdown ADAM10 using an siRNA-mediated method. Cells were pre-treated with 6.2 ng/ml PMA to make them adherent, more megakaryocyte-like, as previously demonstrated (75), and potentially more readily transfectable with siRNA, since suspension cells were not transfectable in preliminary experiments (data not shown). The following day the cells were transfected with 10 nM of control or ADAM10 siRNA or left untransfected. Three days after transfection the cells were stained for ADAM10 and a control (MOPC) using an indirect staining method. Flow cytometry was then used to determine what proportion of ADAM10 remained on the cell surface. A549 cells were transfected with the same siRNAs as a positive control. This cell line was chosen as siRNA knockdown of ADAM10 in these cells had been successfully used by other members of the group (Khan and Tomlinson, unpublished data).

The non-transfected HEL cells and those that had been transfected with control siRNA had similar levels of ADAM10 (Figure 23). However, the cells that had been transfected with ADAM10 siRNA showed only around a 50 % decrease in ADAM10 expression (Figure 23B). Examination of the histogram suggested that this weak knockdown was probably due to poor transfection efficiency, since a small ADAM10-low population was evident in addition to a larger population with normal ADAM10 levels. In contrast, when the A549 cells were transfected with the

ADAM10 siRNA there was a 95 % decrease in the amount of ADAM10 present on the surface of the cells (Figure 24B).

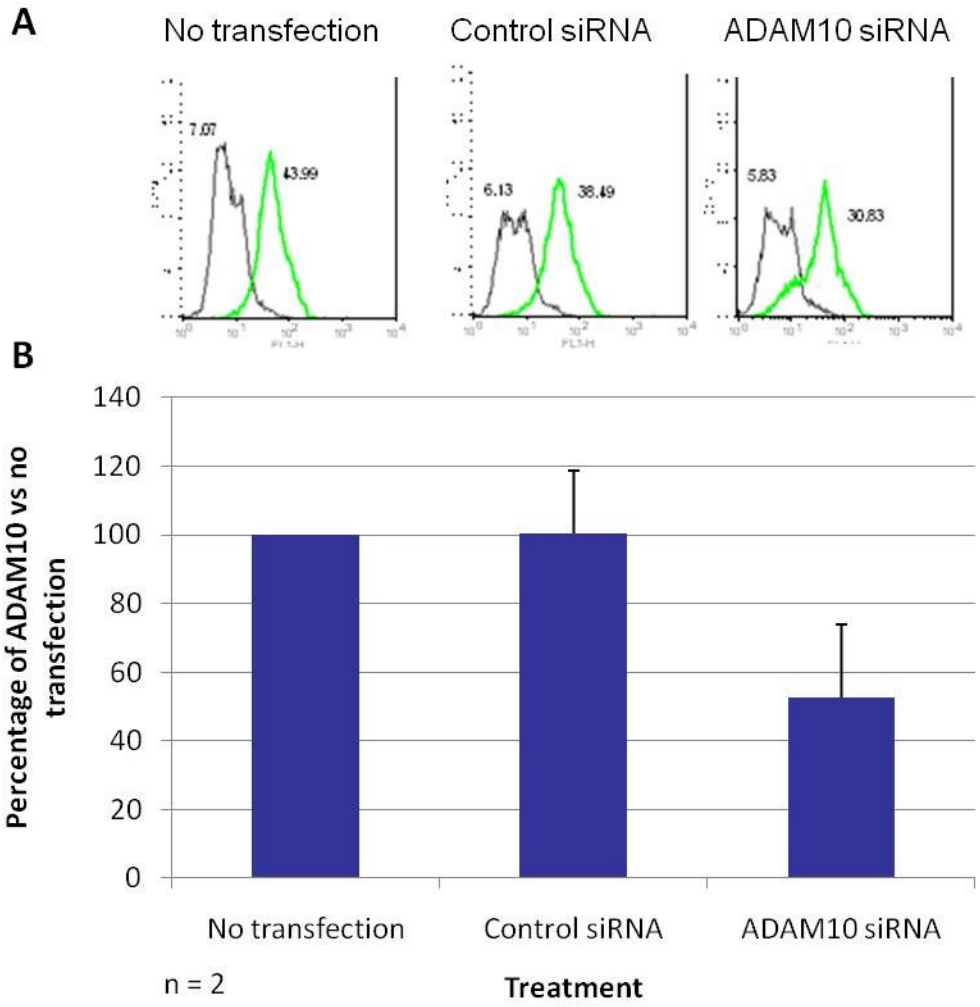

Figure 23: Transfection with ADAM10 siRNA does not significantly reduce ADAM10 on the surface of HEL cells. HEL cells were treated with 6.2 ng/ml PMA to make them more adherent and were transfected with control or ADAM10 siRNA the following day or left untransfected. After 72 hours the amount of ADAM10 on the cells was assessed by flow cytometry, using an indirect staining method. (A) The FACS plots from this experiment do not clearly show a leftward shift of the ADAM10 peak, but there is a shoulder peak forming, which is likely to be the cells in which ADAM10 knockdown has been successful. (B) The amount of ADAM10 after 72 hours was quantified and expressed as a percentage of the amount detected in the non-transfected cells. The control siRNA did not alter the amount of ADAM10. The specific ADAM10 siRNA reduced the amount of ADAM10 by 50 %. Error bars represent the standard deviation of two separate experiments.

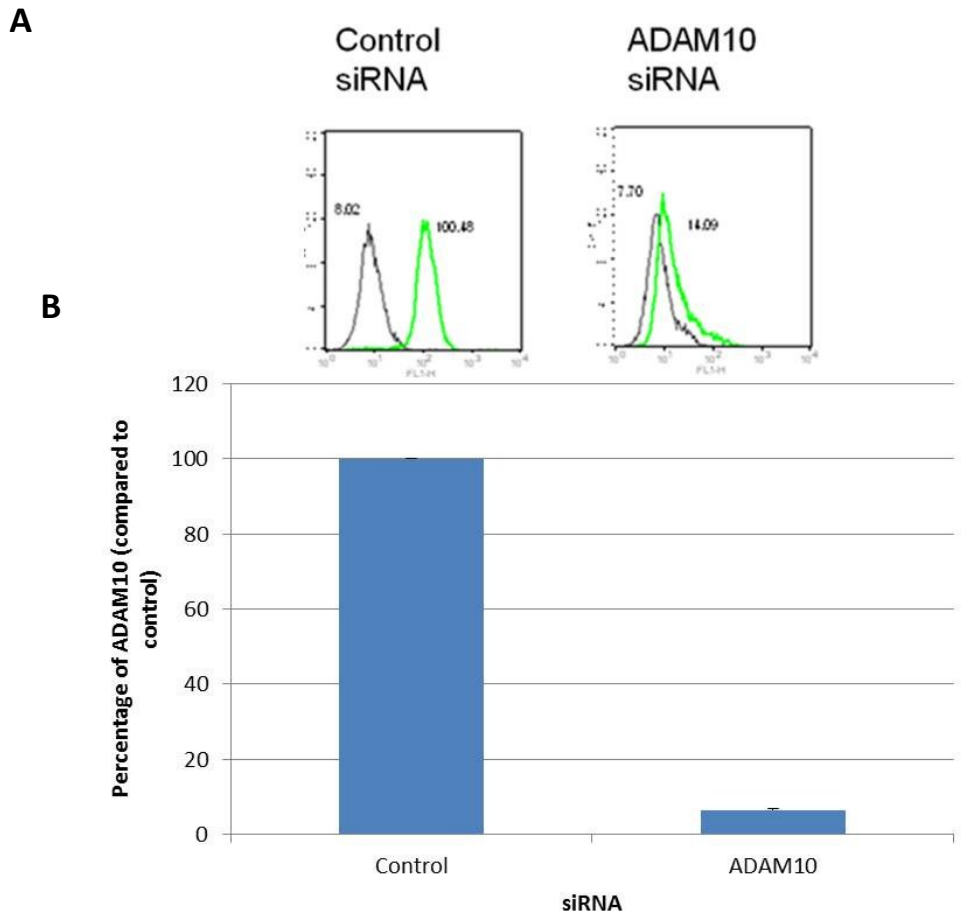

Figure 24: Transfection with ADAM10 siRNA reduces ADAM10 on the surface of A549 cells. A549 cells were transfected with control or ADAM10 siRNA and analysed by flow cytometry 72 hours after transfection. (A) The FACS plot clearly shows the peak representing ADAM10 shifting left after transfection with ADAM10 siRNA. (B) The percentage of ADAM10 after transfection was quantified using the median fluorescence intensity. The specific siRNA gave a reduction of approximately 95 % in this cell line. Error bars represent the standard deviation of two separate experiments.

It is possible that analysing the extent of ADAM10 knockdown 72 hours after transfection was the reason behind the relatively low knockdown levels. At 72 hours the majority of the ADAM10 protein may not have been removed or, alternatively, the HEL cells were beginning to re-express ADAM10 by 72 hours. To determine whether this was affecting the experiment, we carried out a time course study with flow cytometry performed at 48, 72 and 96 hours after transfection. Cells were pre-treated with PMA as in the previous experiment and the transfection used the same siRNA construct. After the appropriate incubation period cells were stained for ADAM10 and a control. The amount of ADAM10 in the cells transfected with specific siRNA was calculated using the median fluorescence intensity and expressed as a percentage of the cells transfected with control siRNA.

The different incubation times did show a difference in ADAM10 expression, but the reduction was not enough to be considered a successful knockdown. After 48 hours there was a 20 % reduction in ADAM10, which became a 10 % reduction after 72 hours (Figure 25). At 96 hours there was a marginal increase in ADAM10 expression. Overall the reduction in ADAM10 in this experiment was lower than that seen previously.

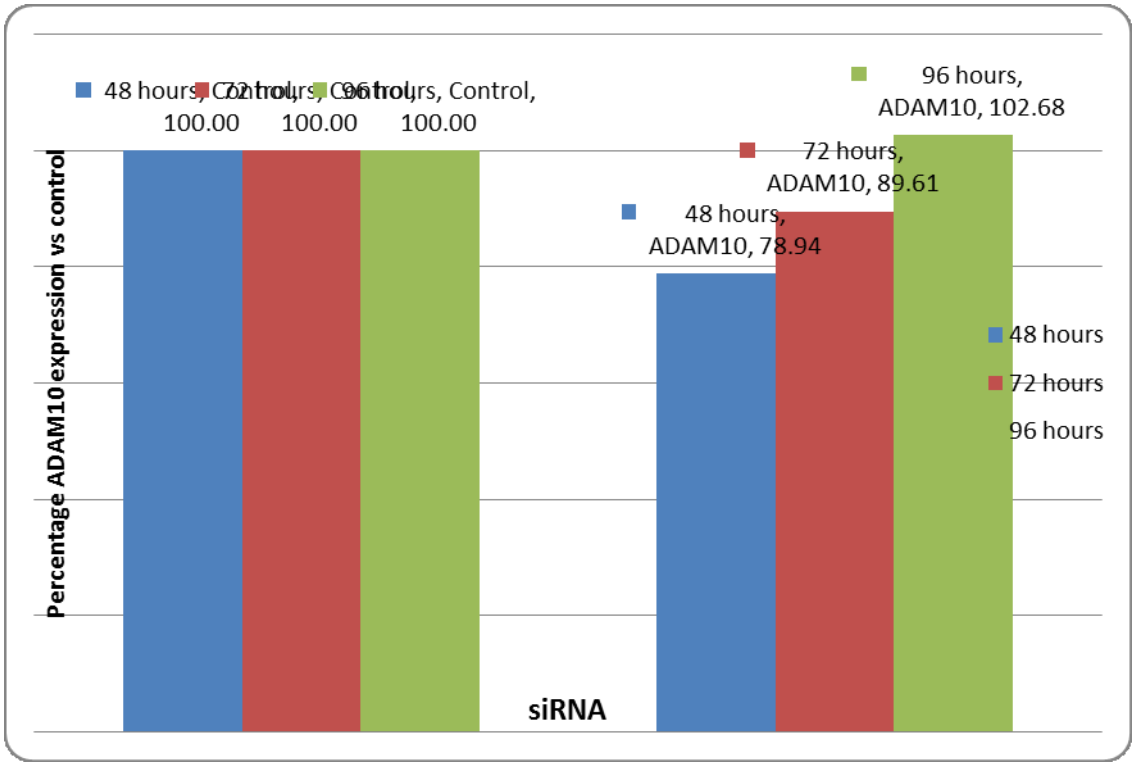

Figure 25: siRNA knockdown of ADAM10 is affected by incubation time. HEL cells were transfected with ADAM10 or control siRNA and ADAM10 expression was determined by flow cytometry at 48, 72 and 96 hours after transfection. The median fluorescence intensity from the FACS plots was normalised and expressed as a percentage of the control sample from the respective time point. There was a 20 % reduction in ADAM10 after 48 hours, which was lost over the following time periods to give a 10 % reduction in ADAM10 after 72 hours and a slight increase in ADAM10 at 96 hours post-transfection. n = 1.

In summary, there was not a significant reduction in ADAM10 at 72 hours post-transfection and the extent of ADAM10 knockdown was not improved when the HEL cells were analysed at 48 and 96 hours. This contrasts to the A549 cells, which gave over 90 % knockdown of ADAM10 with the same siRNA. Together with the low endogenous GPVI expression levels, these data suggest that HEL cells are unlikely to make a good model system in which to study the effects of tetraspanin knockdown on ADAM10 expression and GPVI shedding.

4. DISCUSSION

4.1.Summary of results

The results obtained in the course of this project suggest that ADAM10 is associated with tetraspanins in its resting form as well as when it is activated. Immunoprecipitations combined with neutravidin Western blots have shown that the band pattern characteristic of tetraspanins and their partner proteins can be detected in both CD9 and ADAM10 IPs performed in biotinylated platelets. This is true of samples that were treated with DMSO and W7. In contrast, we were not able to detect the same band pattern in ADAM17 IPs. While W7 and NEM both appear to increase GPVI cleavage in HEL cells, siRNA-mediated knockdown of ADAM10 did not seem to work efficiently in these cells.

4.2.W7 and NEM induce GPVI shedding in platelets

The calmodulin inhibitor W7 and thiol-modifying agent NEM have previously been used as activators of ADAM10 and have been shown to induce GPVI cleavage (53). We confirmed this result using flow cytometry to analyse GPVI levels in PRP and washed platelets after treatment with 150 µM W7, 2mM NEM or a vehicle control. Interestingly, we also found that there was less GPVI staining in the control washed platelets than the PRP. This is believed to be due to the presence of $CaCl_2$ in the Tyrode's buffer that the washed platelets were resuspended in as increasing the intracellular concentration of calcium activates ADAM10 (76). Calcium is chelated during platelet preparation to prevent activation and it is thought that when calcium

was added to the DMSO control the platelets took up the free calcium, increasing the intracellular concentration and activating ADAM10.

Treating platelets with W7 or NEM also increased the levels of CD9 staining. This is thought to be caused by ADAM10-mediated cleavage of other surface proteins in addition to GPVI. It is possible that as the extracellular domains of various proteins were cleaved the CD9 antibodies were more able to access and bind to CD9, therefore increasing the level of staining seen when flow cytometry was performed. This could be confirmed by determining the other targets of ADAM10 on platelets and assessing whether removing these from the platelet surface gave a similar increase in CD9 staining. Identifying ADAM10's target proteins will indicate the size of the extracellular domains being cleaved. Finding that these domains are relatively large will support the theory that CD9 staining is increased after W7 treatment due to the antibody being able to access its target.

4.3.ADAM10 is associated with CD9 in human platelets, irrespective of activation

Immunoprecipitations were used to determine whether ADAM10's association with tetraspanins changes upon activation. Neutravidin Western blots showed that ADAM10 was associated with CD9 after treatment with DMSO as well as after W7 treatment. This, combined with the presence of a CD9 band in both the CD9 and ADAM10 IPs after CD9 Western blotting, suggests that ADAM10 is associated with tetraspanin microdomains irrespective of its activation status. This

result was confirmed by ADAM10 Western blot, which showed a band representing ADAM10 in both the ADAM10 and CD9 IPs. Unlike a previously published study (61), we were not able to detect CD9 in the GPVI IP after neutravidin or CD9 Western blotting. This is thought to be because the blots were developed using an infra-red imaging system, whereas the data obtained by Protty et al. was from a chemiluminescence film blot, which is generally more sensitive than infra-red imaging (Tomlinson et al., unpublished data). It would, therefore, be advisable to repeat the experiment with the blot developed on film to confirm that GPVI is associated with the tetraspanin microdomain.

It was suggested that the presence of calcium ions in the Tyrode's buffer that the platelets were resuspended in may be affecting the assay. Therefore, the experiment was repeated without $CaCl_2$ in the DMSO control, but it was kept in the W7 treatment as calcium ions are necessary for the activation of ADAM10 (77). The neutravidin blots from these repeat experiments still showed that inactive ADAM10 was associated with tetraspanins. Therefore, it can be concluded that while calcium leads to a reduction in surface levels of GPVI it does not affect ADAM10 localisation within the tetraspanin microdomain.

There was also a difference in band intensity between the DMSO-treated and W7-treated samples. Initially, we suspected that this was due to different amounts of protein in the samples, but confirmed that this was not the case and that there were equal amounts of protein. Therefore, we believe that the cleavage of

extracellular domains by ADAM10 makes the remaining non-target platelet proteins more accessible, thus increasing the biotinylation of proteins on W7-treated platelets.

4.4.ADAM17 does not appear to be associated with CD9 in human platelets

There is currently some debate as to whether ADAM17 is associated with CD9, due to conflicting reports published in the last few years (70-72). Immunoprecipitation experiments in biotinylated platelets showed a definite association between ADAM10 and CD9, but suggested that ADAM17 is not associated with CD9. The ADAM17 band was relatively difficult to detect, but was visible when the exposure on the image was increased. Only the IPs performed in Brij97 lysis buffer showed the ADAM10-CD9 association as the Triton X-100 lysis buffer contains a more stringent detergent, which disrupts the tetraspanin microdomain.

Although the data shown here suggests that ADAM17 is not associated with CD9, the possibility that ADAM17 is tetraspanin-associated cannot be completely discarded. CD9 is relatively abundant on the platelet surface, with 45,000 copies (78), so it was thought that any association with ADAM17 would be reasonably easy to detect. However, there is a large deviation between ADAM10 and ADAM17 levels on platelets, with ADAM10 being significantly more abundant as assessed by proteomics (59), and yet the CD9 band in the ADAM10 IP was comparatively weak. Therefore, it is possible that ADAM17 is associated with CD9 but the low levels of

ADAM17 on platelets means the association cannot be detected using this method. To check whether this is the case the experiment should be repeated in a different cell type, preferably one in which ADAM10 and ADAM17 are expressed at similar levels. This difference in ADAM17 expression may also explain why Gutierrez-Lopez (72) reported the association when it had not been detected by other groups (70,71). The other possibility is that the ADAM17 antibody failed to bind properly. To assess this, flow cytometry could be performed using washed platelets to check whether the ADAM17 antibody is binding before repeating the immunoprecipitation experiments.

4.5.W7 and NEM induce GPVI cleavage in HEL cells

One of the aims of this project was to assess whether the megakaryocyte-like HEL cell line would be an appropriate system in which to study the effects of tetraspanins on ADAM10 activity and GPVI cleavage. The first stage in this assessment was to confirm that W7 and NEM were able to activate ADAM10 in these cells. Flow cytometry after incubation with either W7 or NEM showed that GPVI is reduced after treatment with these compounds.

A greater reduction in GPVI was observed with NEM. The reason for this is currently unclear, but it may be that there are other metalloproteinases on the cell surface that are able to cleave GPVI. Matrix metalloproteinases also contain a cysteine switch that regulates their activation, so are likely to be activated by NEM (79), whereas W7 is thought to be a more specific activator of ADAM metalloproteinases, which may result in a lower level of GPVI cleavage compared to

NEM. The GPVI staining intensity was much lower in this experiment than in the earlier platelet experiment. This is probably due to the low cell number that was used in the experiment, which resulted from the presence of a population of dead cells in the samples.

4.6. siRNA-mediated knockdown of ADAM10 is not appropriate for HEL cells

FACS analysis of HEL cells 72 hours after transfection showed only a 50 % reduction in ADAM10 expression. In comparison, A549 cells that were transfected with the same siRNA showed a 95 % reduction in ADAM10 after 72 hours. It was suggested that the disappointing knockdown level was due to the time period at which the cells were assessed: there may have been residual ADAM10 protein or the cells may have begun to re-express ADAM10. To test this, a time course study was performed with analysis of ADAM10 expression at 48, 72 and 96 hours after transfection. However, the ADAM10 knockdown seen in this experiment did not improve on the previously obtained data, suggesting that siRNA transfection is not appropriate for HEL cells.

It is possible that the problem in this experiment was with the transfection reagent rather than the cell line. The transfection was performed using RNAiMAX, which is a lipid-based transfection reagent. It may be prudent to repeat the experiment with a different transfection agent, such as Dharmafect (Thermo Scientific), to see if this improves the transfection efficiency. Alternatively, lentiviral transfection of short hairpin RNA (shRNA) could be used to remove various tetraspanins, but particularly the 8-Cys tetraspanins, from HEL cells. If this is

successful the cells could then be used to study the effect of the removal of these tetraspanins on ADAM10 function.

If the problem was with the cell line, siRNA transfection may be possible in different cell lines. This would allow the interaction between tetraspanins, ADAM10 and GPVI to be studied, but may be different to the situation in platelets and megakaryocytes, which would have to be taken into account when making conclusions from any data that is obtained. In addition to the ADAM10 knockdown not being successful, the GPVI levels in HEL cells were found to be quite low, which could make studying GPVI cleavage difficult. In theory, GPVI cleavage could be studied in primary megakaryocytes, but these are extremely difficult to genetically manipulate. Alternatively, a different cell line could be used, such as the megakaryocyte-like cell lines Dami and MEG-01. There is some debate as to whether these cell lines truly model megakaryocytes. The Dami cell line has been known to be contaminated with the HEL cell line (80) and, like HEL cells, Dami cells can also express erythrocyte markers (81), so may not accurately model megakaryocytes. Comparatively, the phenotype of MEG-01 cells is closer to that of primary megakaryocytes (82), but like all megakaryocytic cell lines is still thought to be biologically different to normal megakaryocytes (83). Both of these cell lines can also be treated with PMA to increase ploidy and make them more megakaryocyte-like (81).

4.7.Conclusions and future directions

The hypothesis behind this project was that the localisation of ADAM10 and GPVI would change when ADAM10 was activated. The specific aims of the project were (i) to determine whether the localisation of ADAM10 changed upon activation; (ii) to confirm whether ADAM17 was associated with CD9 and (iii) to assess whether HEL cells would be a suitable system in which to study the interaction between tetraspanins, ADAM10 and GPVI. The data described above indicate that ADAM10 is associated with tetraspanin microdomains in both its inactive and active forms and that HEL cells may not be the best system in which to study tetraspanins and ADAM10. From the data outlined here it is not possible to conclude whether ADAM17 and CD9 are associated or not.

While we have shown that ADAM10 does not change its localisation upon activation, the experiment should be repeated with the Western blots developed on film to determine whether GPVI is also associated with tetraspanin microdomains both before and after treatment with W7. Further experiments could assess what happens to the remaining section of GPVI after the extracellular domain has been cleaved: does it remain associated with the tetraspanin microdomain?

The immunoprecipitation experiments attempting to show whether ADAM17 is associated with CD9 need to be repeated in a different cell type. In platelets, we were not able to detect the association between ADAM17 and CD9. However, there

is significantly more ADAM10 than ADAM17 on the platelet surface (59), which means that there may not have been enough ADAM17 in the platelet samples to allow the association with CD9 to be detected. Ideally, the cells in which this experiment is repeated should have similar levels of ADAM10 and ADAM17, but platelets are one of few cell types that have had their membrane proteins quantified.

Similarly, more work needs to be undertaken in order to find a suitable cell line in which to study the effect of tetraspanins on ADAM10. The megakaryocyte-like HEL cell line has so far proven difficult to manipulate through siRNA-mediated transfection. These cells may be suitable for lentiviral transfection, but further experiments would be required to confirm this. As previous data has demonstrated that ADAM10 expression is dependent on a number of tetraspanins (70); Collier and Tomlinson, unpublished data), it is possible that ADAM10 regulation by tetraspanins is compensatory. Therefore, lentiviral shRNA knockdowns could be used to assess the effects of a number of tetraspanins on ADAM10 function. In particular, overexpression of Tspan10, Tspan14 or Tspan33 greatly increases levels of mature ADAM10 (Collier and Tomlinson, unpublished data). With this in mind, experiments could knock down these three tetraspanins individually or in combination and assess the effect on ADAM10 cleavage of GPVI.

As well as showing the association between ADAM10 and tetraspanins biochemically, it would be useful to confirm this with imaging techniques. For example, a bioluminescence resonance energy transfer (BRET) assay could be used to

study the interaction in real-time. It would also be interesting to develop a Tspan14 knockout mouse, which would allow the work on tetraspanin regulation of ADAM10 and GPVI to be continued in platelets rather than in a megakaryocyte-like cell line. Tspan14 is the primary tetraspanin on mouse platelets as well as being associated with ADAM10, so the knockout mouse has the potential to have an interesting platelet phenotype.

In summary, ADAM10 is associated with tetraspanins when active and inactive. ADAM17 does not appear to be associated with CD9 in platelets, but this should be confirmed in a different cell type. Finally, HEL cells do not appear to be a suitable model for studying ADAM10 regulation by tetraspanins.

5. REFERENCES

1. Tammela T, Alitalo K. Lymphangiogenesis: Molecular Mechanisms and Future Promise. Cell. 2010;140(4):460-476.

2. Liersch R, Detmar M. Lymphangiogenesis in development and disease. Thrombosis and Haemostasis. 2007;98(2):304-310.

3. Nisato RE, Pepper MS. Lymphatic endothelial cells: establishment of primaries and characterization of established lines. In: Angiogenesis Protocols. 2008. p. 113-126.

4. Wigle JT, Oliver G. Prox1 function is required for the development of the murine lymphatic system. Cell. 1999;98(6):769-778.

5. Wigle JT, Harvey N, Detmar M, Lagutina I, Grosveld G, Gunn MD, et al. An essential role for Prox1 in the induction of the lymphatic endothelial cell phenotype. EMBO Journal. 2002;21(7):1505-1513.

6. Oliver G, Detmar M. The rediscovery of the lymphatic system: Old and new insights into the development and biological function of the lymphatic vasculature. Genes and Development. 2002;16(7):773-783.

7. Oliver G, Harvey N. A stepwise model of the development of the lymphatic vasculature. 2002. p. 159-165.

8. Oliver G, Srinivasan RS. Lymphatic vasculature development: Current concepts. In: Lymphatic vasculature development: Current concepts. 2008. p. 75-81.

9. Carmeliet P. Mechanisms of angiogenesis and arteriogenesis. Nature Medicine. 2000;6(4):389-395.

10. Kukk E, Lymboussakl A, Taira S, Kaipainen A, Jeltsch M, Joukov V, et al. VEGF-C receptor binding and pattern of expression with VEGFR-3 suggests a role in lymphatic vascular development. Development. 1996;122(12):3829-3837.

11. Mäkinen T, Veikkola T, Mustjoki S, Karpanen T, Catimel B, Nice EC, et al. Isolated lymphatic endothelial cells transduce growth, survival and migratory signals via the VEGF-C/D receptor VEGFR-3. EMBO Journal. 2001;20(17):4762-4773.

12. Karkkainen MJ, Haiko P, Sainio K, Partanen J, Taipale J, Petrova TV, et al. Vascular endothelial growth factor C is required for sprouting of the first lymphatic vessels from embryonic veins. Nature Immunology. 2004;5(1):74-80.

13. Baluk P, Tammela T, Ator E, Lyubynska N, Achen MG, Hicklin DJ, et al. Pathogenesis of persistent lymphatic vessel hyperplasia in chronic airway inflammation. Journal of Clinical Investigation. 2005;115(2):247-257.

14. Lamalice L, Le Boeuf F, Huot J. Endothelial cell migration during angiogenesis. Circulation Research. 2007;100(6):782-794.

15. Tammela T, Enholm B, Alitalo K, Paavonen K. The biology of vascular endothelial growth factors. Cardiovascular Research. 2005;65(3):550-563.

16. Oliver G. Lymphatic vasculature development. Nature Reviews Immunology. 2004;4(1):35-45.

17. Alitalo K, Tammela T, Petrova TV. Lymphangiogenesis in development and human disease. Nature. 2005;438(7070):946-953.

18. Maby-El Hajjami H, Petrova TV. Developmental and pathological lymphangiogenesis: From models to human disease. Histochemistry and Cell Biology. 2008;130(6):1063-1078.

19. Schoppmann SF, Birner P, Stöckl J, Kalt R, Ullrich R, Caucig C, et al. Tumor-associated macrophages express lymphatic endothelial growth factors and are related to peritumoral lymphangiogenesis. American Journal of Pathology. 2002;161(3):947-956.

20. Breiteneder-Geleff S, Soleiman A, Kowalski H, Horvat R, Amann G, Kriehuber E, et al. Angiosarcomas express mixed endothelial phenotypes of blood and lymphatic capillaries: Podoplanin as a specific marker for lymphatic endothelium. American Journal of Pathology. 1999;154(2):385-394.

21. Schacht V, Ramirez MI, Hong Y-K, Hirakawa S, Feng D, Harvey N, et al. T1α/podoplanin deficiency disrupts normal lymphatic vasculature formation and causes lymphedema. EMBO Journal. 2003;22(14):3546-3556.

22. Uhrin P, Zaujec J, Breuss JM, Olcaydu D, Chrenek P, Stockinger H, et al. Novel function for blood platelets and podoplanin in developmental separation of blood and lymphatic circulation. Blood. 2010;115(19):3997-4005.

23. Fu J, Gerhardt H, McDaniel JM, Xia B, Liu X, Ivanciu L, et al. Endothelial cell O-glycan deficiency causes blood/lymphatic misconnections and consequent fatty liver disease in mice. Journal of Clinical Investigation. 2008;118(11):3725-3737.

24. Martín-Villar E, Megías D, Castel S, Yurrita MM, Vilaró S, Quintanilla M. Podoplanin binds ERM proteins to activate RhoA and promote epithelial-mesenchymal transition. Journal of Cell Science. 2006;119(21):4541-4553.

25. Sakabe M, Ikeda K, Nakatani K, Kawada N, Imanaka-Yoshida K, Yoshida T, et al. Rho kinases regulate endothelial invasion and migration during valvuloseptal endocardial cushion tissue formation. Developmental Dynamics. 2006;235(1):94-104.

26. Amano M, Chihara K, Kimura K, Fukata Y, Nakamura N, Matsuura Y, et al. Formation of actin stress fibers and focal adhesions enhanced by Rho- kinase. Science. 1997;275(5304):1308-1311.

27. Van Nieuw Amerongen GP, Koolwijk P, Versteilen A, Van Hinsbergh VWM. Involvement of RhoA/Rho kinase signaling in VEGF-induced endothelial cell migration and angiogenesis in vitro. Arteriosclerosis, Thrombosis, and Vascular Biology. 2003;23(2):211-217.

28. Navarro A, Perez RE, Rezaiekhaligh MH, Mabry SM, Ekekezie II. Polarized migration of lymphatic endothelial cells is critically dependent on podoplanin regulation of Cdc42. American Journal of Physiology - Lung Cellular and Molecular Physiology. 2011;300(1):L32-L42.

29. Abtahian F, Guerriero A, Sebzda E, Lu M-M, Zhou R, Mocsai A, et al. Regulation of blood and lymphatic vascular separation by signaling proteins SLP-76 and Syk. Science. 2003;299(5604):247-251.

30. Bertozzi CC, Schmaier AA, Mericko P, Hess PR, Zou Z, Chen M, et al. Platelets regulate lymphatic vascular development through CLEC-2-SLP-76 signaling. Blood. 2010;116(4):661-670.

31. Ichise H, Ichise T, Ohtani O, Yoshida N. Phospholipase Cγ2 is necessary for separation of blood and lymphatic vasculature in mice. Development. 2009;136(2):191-195.

32. Christou CM, Pearce AC, Watson AA, Mistry AR, Pollitt AY, Fenton-May AE, et al. Renal cells activate the platelet receptor CLEC-2 through podoplanin. Biochemical Journal. 2008;411(1):133-140.

33. Suzuki-Inoue K, Kato Y, Inoue O, Mika KK, Mishima K, Yatomi Y, et al. Involvement of the snake toxin receptor CLEC-2, in podoplanin-mediated platelet activation, by cancer cells. Journal of Biological Chemistry. 2007;282(36):25993-26001.

34. Suzuki-Inoue K, Fuller GLJ, García Á, Eble JA, Pöhlmann S, Inoue O, et al. Anovel Syk-dependent mechanism of platelet activation by the C-type lectin receptor CLEC-2. Blood. 2006;107(2):542-549.

35. Hughes CE, Pollitt AY, Mori J, Eble JA, Tomlinson MG, Hartwig JH, et al. CLEC-2 activates Syk through dimerization. Blood. 2010;115(14):2947-2955.

36. Kerrigan AM, Dennehy KM, Mourão-Sá D, Faro-Trindade I, Willment JA, Taylor PR, et al. CLEC-2 is a phagocytic activation receptor expressed on murine peripheral blood neutrophils. Journal of Immunology. 2009;182(7):4150-4157.

37. O'Callaghan CA. Thrombomodulation via CLEC-2 targeting. Current Opinion in Pharmacology. 2009;9(2):90-95.

38. Wicki A, Christofori G. The potential role of podoplanin in tumour invasion. British Journal of Cancer. 2007;96(1):1-5.

39. Suzuki-Inoue K, Inoue O, Ding G, Nishimura S, Hokamura K, Eto K, et al. Essential in vivo roles of the C-type lectin receptor CLEC-2: Embryonic/neonatal lethality of CLEC-2-deficient mice by blood/lymphatic misconnections and impaired thrombus formation of CLEC-2-deficient platelets. Journal of Biological Chemistry. 2010;285(32):24494-24507.

40. Imoukhuede PI, Popel AS. Quantification and cell-to-cell variation of vascular endothelial growth factor receptors. Exp Cell Res. 2011 Apr 15;317(7):955-965.

41. Kato Y, Kaneko MK, Kuno A, Uchiyama N, Amano K, Chiba Y, et al. Inhibition of tumor cell-induced platelet aggregation using a novel anti-podoplanin antibody reacting with its platelet-aggregation-stimulating domain. Biochemical and Biophysical Research Communications. 2006 Nov 3;349(4):1301-1307.

42. Charrin S, Le Naour F, Silvie O, Milhiet P-E, Boucheix C, Rubinstein E. Lateral organization of membrane proteins: Tetraspanins spin their web. Biochemical Journal. 2009;420(2):133-154.

43. André M, Le Caer J-P, Greco C, Planchon S, El Nemer W, Boucheix C, et al. Proteomic analysis of the tetraspanin web using LC-ESI-MS/MS and MALDI-FTICR-MS. Proteomics. 2006;6(5):1437-1449.

44. Levy S, Shoham T. The tetraspanin web modulates immune-signalling complexes. Nature Reviews Immunology. 2005;5(2):136-148.

45. Rubinstein E, Naour FL, Lagaudrière-Gesbert C, Billard M, Conjeaud H, Boucheix C. CD9, CD63, CD81, and CD82 are components of a surface tetraspan network connected to HLA-DR and VLA integrins. European Journal of Immunology. 1996;26(11):2657-2665.

46. Krementsov DN, Rassam P, Margeat E, Roy NH, Schneider-Schaulies J, Milhiet P-E, et al. HIV-1 assembly differentially alters dynamics and partitioning of tetraspanins and raft components. Traffic. 2010;11(11):1401-1414.

47. Hemler ME. Tetraspanin functions and associated microdomains. Nature Reviews Molecular Cell Biology. 2005;6(10):801-811.

48. Boucheix C. Severely reduced female fertility in CD9-deficient mice. Science. 2000;287(5451):319-321.

49. Kaji K, Oda S, Miyazaki S, Kudo A. Infertility of CD9-deficient mouse eggs is reversed by mouse CD9, human CD9, or mouse CD81; polyadenylated mRNA injection developed for molecular analysis of sperm-egg fusion. Developmental Biology. 2002;247(2):327-334.

50. Takeda Y, He P, Tachibana I, Zhou B, Miyado K, Kaneko H, et al. Double Deficiency of Tetraspanins CD9 and CD81 Alters Cell Motility and Protease Production of Macrophages and Causes Chronic Obstructive Pulmonary Disease-like Phenotype in Mice. Journal of Biological Chemistry. 2008;283(38):26089 -26097.

51. Boucheix C, Rubinstein E. Tetraspanins. Cell. Mol. Life Sci. 2001 Aug;58(9):1189-1205.

52. Seigneuret M, Delaguillaumie A, Lagaudrière-Gesbert C, Conjeaud H. Structure of the tetraspanin main extracellular domain. A partially conserved fold with a structurally variable domain insertion. J. Biol. Chem. 2001 Oct 26;276(43):40055-40064.

53. Gardiner EE, Karunakaran D, Shen Y, Arthur JF, Andrews RK, Berndt MC. Controlled shedding of platelet glycoprotein (GP)VI and GPIb-IX-V by ADAM family metalloproteinases. Journal of Thrombosis and Haemostasis. 2007;5(7):1530-1537.

54. Bender M, Hofmann S, Stegner D, Chalaris A, Bösl M, Braun A, et al. Differentially regulated GPVI ectodomain shedding by multiple platelet-expressed proteinases. Blood. 2010;116(17):3347-3355.

55. Lau L-M, Wee JL, Wright MD, Moseley GW, Hogarth PM, Ashman LK, et al. The tetraspanin superfamily member CD151 regulates outside-in integrin alphaIIbbeta3 signaling and platelet function. Blood. 2004 Oct 15;104(8):2368-2375.

56. Goschnick MW, Lau L-M, Wee JL, Liu YS, Hogarth PM, Robb LM, et al. Impaired “outside-in” integrin αIIbβ 3 signaling and thrombus stability in TSSC6-deficient mice. Blood. 2006;108(6):1911-1918.

57. Tomlinson MG. Platelet tetraspanins: small but interesting. Journal of Thrombosis and Haemostasis. 2009 Dec 1;7(12):2070-2073.

58. Haining EJ, Yang J, Tomlinson MG. Tetraspanin microdomains: Fine-tuning platelet function. Biochemical Society Transactions. 2011;39(2):518-523.

59. Lewandrowski U, Wortelkamp S, Lohrig K, Zahedi RP, Wolters DA, Walter U, et al. Platelet membrane proteomics: A novel repository for functional research. Blood. 2009;114(1):e10-e19.

60. Goschnick MW, Jackson DE. Tetraspanins-structural and signalling scaffolds that regulate platelet function. Mini Rev Med Chem. 2007 Dec;7(12):1248-1254.

61. Protty MB, Watkins NA, Colombo D, Thomas SG, Heath VL, Herbert JMJ, et al. Identification of Tspan9 as a novel platelet tetraspanin and the collagen receptor GPVI as a component of tetraspanin microdomains. Biochem. J. 2009 Jan 1;417(1):391-400.

62. Watson SP, Asazuma N, Atkinson B, Berlanga O, Best D, Babe R, et al. The role of ITAM-and ITIM-coupled receptors in platelet activation by collagen. Thrombosis and Haemostasis. 2001;86(1):276-288.

63. Wolfsberg TG, Bazan JF, Blobel CP, Myles DG, Primakoff P, White JM. The precursor region of a protein active in sperm-egg fusion contains a metalloprotease and a disintegrin domain: Structural, functional, and evolutionary implications. Proceedings of the National Academy of Sciences of the United States of America. 1993;90(22):10783-10787.

64. Fahrenholz F, Gilbert S, Kojro E, Lammich S, Postina R. α-Secretase activity of the disintegrin metalloprotease ADAM 10: Influences of domain structure. 2000. p. 215-222.

65. Anders A, Gilbert S, Garten W, Postina R, Fahrenholz F. Regulation of the alpha-secretase ADAM10 by its prodomain and proprotein convertases. The FASEB journal : official publication of the Federation of American Societies for Experimental Biology. 2001;15(10):1837-1839.

66. Sahin U, Weskamp G, Kelly K, Zhou H-M, Higashiyama S, Peschon J, et al. Distinct roles for ADAM10 and ADAM17 in ectodomain shedding of six EGFR ligands. Journal of Cell Biology. 2004;164(5):769-779.

67. Pan D, Rubin GM. Kuzbanian controls proteolytic processing of Notch and mediates lateral inhibition during Drosophila and vertebrate neurogenesis. Cell. 1997 Jul 25;90(2):271-280.

68. Lammich S, Kojro E, Postina R, Gilbert S, Pfeiffer R, Jasionowski M, et al. Constitutive and regulated α-secretase cleavage of Alzheimer's amyloid precursor protein by a disintegrin metalloprotease. Proceedings of the National Academy of Sciences of the United States of America. 1999;96(7):3922-3927.

69. Kojro E, Fahrenholz F. The non-amyloidogenic pathway: structure and function of alpha-secretases. Subcell. Biochem. 2005;38:105-127.

70. Arduise C, Abache T, Li L, Billard M, Chabanon A, Ludwig A, et al. Tetraspanins regulate ADAM10-mediated cleavage of TNF-alpha and epidermal growth factor. J. Immunol. 2008 Nov 15;181(10):7002-7013.

71. Xu D, Sharma C, Hemler ME. Tetraspanin12 regulates ADAM10-dependent cleavage of amyloid precursor protein. FASEB J. 2009 Nov;23(11):3674-3681.

72. Gutiérrez-López MD, Gilsanz A, Yáñez-Mó M, Ovalle S, Lafuente EM, Domínguez C, et al. The sheddase activity of ADAM17/TACE is regulated by the tetraspanin CD9. Cellular and Molecular Life Sciences: CMLS. 2011;

73. Andrews RK, Suzuki-Inoue K, Shen Y, Tulasne D, Watson SP, Berndt MC. Interaction of calmodulin with the cytoplasmic domain of platelet glycoprotein VI. Blood. 2002;99(11):4219-4221.

74. André M, Chambrion C, Charrin S, Soave S, Chaker J, Boucheix C, et al. In situ chemical cross-linking on living cells reveals CD9P-1 cis-oligomer at cell surface. Journal of Proteomics. 2009;73(1):93-102.

75. Berlanga O, Bobe R, Becker M, Murphy G, Leduc M, Bon C, et al. Expression of the collagen receptor glycoprotein VI during megakaryocyte differentiation. Blood. 2000;96(8):2740-2745.

76. Nagano O, Murakami D, Hartmann D, De Strooper B, Saftig P, Iwatsubo T, et al. Cell-matrix interaction via CD44 is independently regulated by different metalloproteinases activated in response to extracellular Ca2+ influx and PKC activation. Journal of Cell Biology. 2004;165(6):893-902.

77. Le Gall SM, Bobé P, Reiss K, Horiuchi K, Niu XD, Lundell D, et al. ADAMs 10 and 17 represent differentially regulated components of a general shedding machinery for membrane proteins such as transforming growth factor alpha, L-selectin, and tumor necrosis factor alpha. Molecular biology of the cell. 2009;20(6):1785-1794.

78. Senis YA, Tomlinson MG, García Á, Dumon S, Heath VL, Herbert J, et al. A comprehensive proteomics and genomics analysis reveals novel transmembrane proteins in human platelets and mouse megakaryocytes including G6b-B, a novel immunoreceptor tyrosine-based inhibitory motif protein. Molecular and Cellular Proteomics. 2007;6(3):548-564.

79. Andrews RK, Karunakaran D, Gardiner EE, Berndt MC. Platelet receptor proteolysis: A mechanism for downregulating platelet reactivity. Arteriosclerosis, Thrombosis, and Vascular Biology. 2007;27(7):1511-1520.

80. MacLeod R, Dirks WG, Reid YA, Hay RJ, Drexler HG. Identity of original and late passage Dami megakaryocytes with HEL erythroleukemia cells shown by combined cytogenetics and DNA fingerprinting. Leukemia. 1997;11(12):2032-2038.

81. Saito H. 3 Megakaryocytic cell lines. Baillière's Clinical Haematology. 1997 Feb;10(1):47-63.

82. Ogura M, Morishima Y, Ohno R. Establishment of a novel human megakaryoblastic leukemia cell line, MEG-01, with positive Philadelphia chromosome. Blood. 1985;66(6):1384-1392.

83. Hoffman R. Regulation of megakaryocytopoiesis. Blood. 1989;74(4):1196-1212.